

*SYNTHESIS AND CHARACTERIZATION OF IRON OXIDE
NANOPARTICLES EMBEDDED ON VARIOUS POLYMERS*



UNIVERSITY of the
WESTERN CAPE



By

Siphesihle Magqazolo

A minithesis submitted in partial fulfilment of the requirements for the degree
of:

Magister Scientiae in Nanoscience

Faculty of Natural Science

University of the Western Cape,

Cape Town, South Africa

Supervisor: Prof. Martin Onani

DECLARATION

I declare that the Synthesis and characterization Iron oxide nanoparticles embedded on various polymers is my own work, that it has not been submitted before for any degree or examination in any other university, and that all the sources I have used or quoted have been indicated and acknowledged as complete references.

Siphesihle Magqazolo

Signature:

Date:



\

DEDICATION

I dedicate my MSc monograph to my mother Sandiswa Nomdatya and my two brothers Samora Magqazolo and Phumelela Magqazolo, who have been my support system throughout my studies, your love and support means the world to me.



UNIVERSITY *of the*
WESTERN CAPE

ACKNOWLEDGEMENTS

I would like to acknowledge the following people or institutions:

- My supervisor Prof Martin Onani from the University of the Western Cape who has assisted me throughout both as a researcher and personally without his support I would be nowhere towards the finish line
- The Organometallics and Nanomaterials group from the University of the Western Cape for all the support and assistance during the time I have spent with them
- Special thanks to Lungisa Lotha, Kiplagaat Ayabei and Garvin Allard for all the support and advice
- The XRD group at iThemba LABSs, Physics department at the University of the Western Cape for allowing me access to their instruments and giving advice about the results I got.
- Prof Andre Strydom from the University of Johannesburg for the SQUID analysis
- Prof Titinchi from the University of the Western Cape for TGA analysis
- Mrs Valencia Jamalie for all the assistance with regards to admin and her office



ABSTRACT

During the course of this study iron oxide nanoparticles, which have been researched for drug-targeted delivery, were synthesised via the co-precipitation method and characterised using various methods. This study focused on the role of relevant capping agents for the inhibition of agglomeration of the particles; chitosan, polyvinyl alcohol (PVA) and poly lactic glycolic acid (PLGA) were the capping agents of interest. The study is an assessment of the effects brought about the different capping agents used for this work. The prepared particles were then capped with the different capping agents followed by the loading of the drug curcumin. Various analytical methods were used to analyse the particles such as High resolution transmission electron microscopy (HR-TEM), Superconducting quantum interference device (SQUID), Fourier Transform Infrared spectroscopy (FT-IR), X-ray diffraction (XRD), Thermogravimetric analysis (TGA) and zeta potential. PVA, chitosan and PLGA capped SPIONS were successfully prepared and verified by FT-IR spectrometry, various sizes were prepared almost ranging the same for the successfully prepared particles verified by XRD. The resultant particles were found to be spherical with an average particles size between 13- 22 nm. From the study it was concluded that the addition of the different capping agents resulted in the reduction of the intensity of the peaks in XRD, it was also found out the presence of the capping agents did not alter the crystalline phase of the particles. From the study it was also observed that higher saturation magnetization was experienced where PVA was used as the capping agents.

Keywords: Iron oxide nanoparticles, Superparamagnetic, Superparamagnetic iron oxide nanoparticles, Co-precipitation, Capping agents, Polyvinyl alcohol, PLGA, Chitosan, Curcumin, Drug loading, Targeted drug deliver

ABBREVIATIONS AND SYMBOLS

SPIONS	Superparamagnetic Iron oxide nanoparticles
PLGA	Poly lactic glycolic acid
PVA	Poly vinyl alcohol
HR-TEM	High resolution transmission electron microscopy
XRD	X-ray diffraction
EDS	Energy dispersive X-ray spectroscopy
SQUID	Superconducting quantum interference device
TGA	Thermogravimetric analysis
FTIR	Fourier Transform Infrared spectroscopy
Bare nanoparticles	uncapped with polymer
OC	Degrees Celsius
Min	Minutes
CVD	Chemical vapour deposition
ECD	Electro deposition
MRI	Magnetic resonance imaging
JCPDS	Joint committee of Diffraction Patterns Standards
FESEM	High-resolution field emission scanning electron microscopy
NPs	Nanoparticles
IONPs	iron oxide nanoparticles
GA	Glycyrrhizic acid
GAIONPs	Glycyrrhizic acid iron oxide nanoparticles
MIC	Minimum inhibitory concentration
PVP	polyvinylpyrrolidone

∅

Diameter

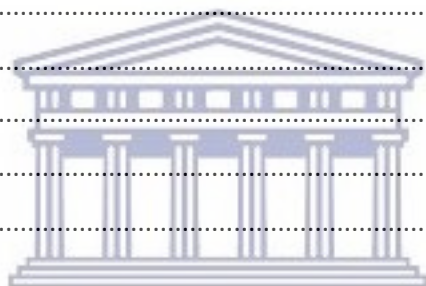


UNIVERSITY *of the*
WESTERN CAPE

Table of Contents

DECLARATION	ii
DEDICATION	iii
ACKNOWLEDGEMENTS	iv
ABSTRACT.....	v
ABBREVIATIONS AND SYMBOLS	vi
LIST OF FIGURES	x
LIST OF TABLES	xii
Chapter 1.....	1
1.1 Introduction.....	1
1.2 Iron oxide nanomaterials.....	1
1.3 Cancer	3
1.4 Capping agents.....	4
1.5 Research aims and objectives	5
Chapter 2.....	7
2.1 Literature review	7
2.2 Synthetic routes.....	14
2.2.1 Hydrothermal	14
2.2.2 Chemical vapour deposition (CVD) and electro deposition (ECD).....	15
2.2.3 High temperature (Thermal) decomposition.....	16
2.2.4 Co-precipitation	17
2.3 Surface coating.....	18
2.3.1 Au coating.....	18
2.3.2 Polymer coating	19
2.3.3 Carbon coating	22
2.3.4 Drug loading	23
Chapter 3.....	25
3.1 Methodology	25
3.1.1 Chemicals.....	25
3.1.1 Synthesis	25
3.1.2 Uncapped nanoparticles	25
3.1.3 Chitosan capped particles.....	26
3.1.4 PVA capped particles.....	26
3.1.5 PLGA capped particles	26
3.1.6 Drug loading	26

3.1	Characterization techniques	27
3.1.1	FITR.....	27
3.1.2	XRD	28
3.1.3	HRTEM.....	29
3.1.4	SQUID	30
3.1.5	TGA	30
Chapter 4.....		32
4.1	Results and discussion	32
4.1.1	HRTEM.....	32
4.1.2	FTIR.....	35
4.1.3	Zeta potential	36
4.1.4	XRD results.....	37
4.1.5	SQUID	39
4.1.6	TGA	41
Chapter 5.....		43
5.1	Conclusion	43
5.2	Future work.....	43
5.3	References.....	44



UNIVERSITY *of the*
WESTERN CAPE

LIST OF FIGURES

FIGURE	PAGE
Figure 1: Things to consider when preparing SPIONS	2
Figure 2: Typical representation of SPIONS capped and loaded	3
Figure 3: FESEM and TEM micrograph of iron oxide nanoparticles prepared via the green method	7
Figure 4: SEM images of (a) iron oxide nanoparticles without magnetic field and (b) with magnetic field	8
Figure 5: Magnetization curves and XRD patterns of both chitosan capped nanoparticles prepared under magnetic field and without	9
Figure 6: (a) XRD pattern of GAIONPs, (b) Fourier transform infrared spectra of (i) IONPs, (ii) GAIONPs and (iii) GA, (c) TG/DTA analysis for GAIONPs. Inset: TG analysis comparative curves	9
Figure 7: XRD patterns for IONPs (a) without PVP and (b) with PVP	11
Figure 8: TGA curve of IONPs without PVP and with PVP	11
Figure 9: SEM micrographs of IONPs (a & b) without PVP and (c and d) with PVP	12
Figure 10: A depiction of the (A) TEM micrograph of capped SPION, (B) TGA curve of a. uncapped SPION, b. capped SPIONS and (C) XRD patterns of the uncapped and capped particles	13
Figure 11: Average particles size and Zeta potential	13
Figure 12: Chemical structure of chitosan	20
Figure 13: Chemical representation of PVA	22
Figure 14: PLGA chemical structure	22
Figure 15: (a) Chemical structure of curcumin and (b) FTIR representation of curcumin	24
Figure 16: Typical FT-IR setup	27
Figure 17: Typical setup of XRD	29
Figure 18: Typical HRTEM interaction with sample	29
Figure 19: Schematic working of SQUID	30
Figure 20: Typical representation of TGA curve	31
Figure 21: (a) Uncapped SPION nanoparticles (b) chitosan capped SPION particles	32

Figure 22: Particle distribution histograms	33
Figure 23: (a) PLGA capped SPION nanoparticles (b) PVA capped SPION nanoparticles	33
Figure 24: Particle size distribution of PVA capped SPIONS	33
Figure 25: Fourier transform spectrum of uncapped and loaded particles with CCM	35
Figure 26: Capped and loaded with curcumin SPIONS	36
Figure 27: Zeta potential of SPIONS	37
Figure 28: X-ray diffraction representation of various SPIONS	38
Figure 29: Depiction of magnetism of the particles	40
Figure 30: TGA curve of SPIONS depicting the decomposition of the particles	41



LIST OF TABLES

Table 1: Determination of particle size by Scherer equation

38



Chapter 1

Chapter overview

This chapter serves as an introduction to nanoscience and SPIONS. The project problem statement and objectives are also outlined.

1.1 Introduction

The field of nanoscience/nanotechnology defined as the study and manipulation of materials at nanoscale, has improved over the past decades as new materials and methods have been developed to solve various problems in different fields. Nano sized materials have been extensively researched due to their properties which enable them to be tailor made specifically for the designated uses, these properties are merely due to their size. These properties include higher strength, lighter weight, increased control of light spectrum, increased chemical reactivity than their larger-scale counterparts and large surface area brought about the size of these materials. Therefore, permitting the attachment of various materials i.e. polymers, drugs, proteins etc. to the surface of these material.(1) Graphene sheets, carbon nanotubes, nano dots are some of the nano materials of current interest in various fields such as polymer, lithium ion batteries, magnetic separation, chemistry, biomedical industry etc.(2)

1.2 Iron oxide nanomaterials

Super paramagnetic iron oxide nanoparticles (SPIONs) are magnetic nanoparticles that are based on magnetite (Fe_3O_4)(3). These magnetic nanoparticles offer new and exciting opportunities for the development of effective drug delivery systems, as they are easy to fabricate, characterize and tailor their properties for various applications (4). Some of the applications include the use of nano probes for in vivo imaging, contrast agents in magnetic resonance imaging(5), immobilization of enzyme, magnetisable implants for targeted drug delivery, stimuli-responsive systems, methanol decomposition catalysis, hyperthermia treatments, environmental analysis and magnetic separations (6)(7) (4).

One of the most important properties of these nanoparticles is that they are super paramagnetic this brought about the application of a magnetic field to the nanoparticles (5). Therefore, nanoparticles are not permanently magnetic thus as soon as the magnetic field is turned off the magnetic property of the SPIONS is impassive therefore the magnetic field may be used to manipulate the direction of the particles. The large surface area associated with these particles enables the attachment of various materials to them, therefore giving rise to the abundant applications associated with these particles (4).

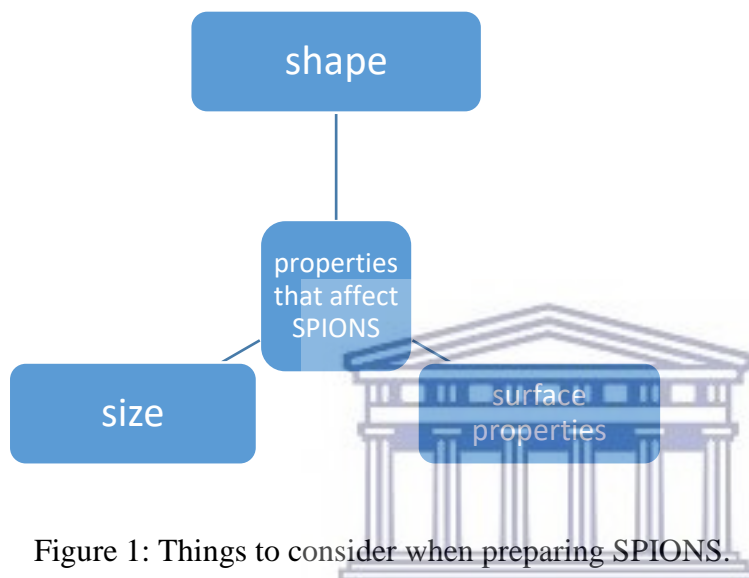


Figure 1: Things to consider when preparing SPIONS.

An example of the applications of these particles is the detection of cancer cells. This was accomplished by conjugating the particles with specific antibodies followed by the transportation of the particles to the body organ that may be affected with cancer. The antibody will detect the presence of cancer via antigens produced by cancer, this can help with early detection of cancer and early treatment as cancer is usually detected in its later stages this triggering difficulties in the treatment usually resulting in the victims death (8).

Polymeric compounds that are hydrophilic in nature are used as capping agents to inhibit agglomeration between the SPIONS, as they tend to react in a dipole-dipole manner in solution. The hydrophilic nature of these capping agents is due to the presence of chemical groups such as $-COOH$, $-NH_2$, $-OH$ etc. in their backbone. These groups aiding to the insolubility of the SPIONS, therefore they can be utilized in the human body, which comprises of about 70 percent of water. The molecule formed when the capping agent reacts with SPIONS retains both characteristics of the agent as well as that of the nanoparticle. The capping agent of choice must be non-toxic as well as biocompatible, as the SPIONS are

predominantly utilized for bio molecular applications. Therefore, magnetic nanoparticles having the above mentioned characteristics are highly compatible to bind to enzymes, proteins, nucleotides etc. aiding to many applications as they are highly reactive (9).

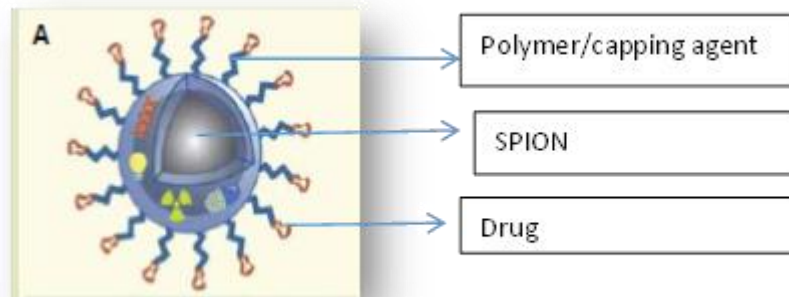


Figure 2: Typical representation of SPIONs capped and loaded.

SPIONs have been synthesized using various methods such as hydrothermal method, microwave, co-precipitation method etc. with co-precipitation being the most used method as it is relatively cheap, produces high yield and uses readily available reactants,(10)(2) therefore co-precipitation method was used for this work (11).

1.3 Cancer

Cancer is a deadly disease initiated by the abnormal growth of cells within the human body making it difficult to control the growth of these cells. Unhealthy lifestyles such as smoking, excess alcohol consumption, malnutrition are some of the causes of cancer. Cancer may be prevented by various changes in lifestyle such as stopping smoking, low alcohol consumption as well as living a healthy lifestyle such as eating healthy food and exercising. In some cases, where the main cause is hereditary genetic mutations, there is no prevention but a healthy lifestyle would reduce the risks and severity of the cancer (2)(3).

Statistics have indicated that cancer ends lives daily due to some of the drawbacks associated with the treatment of cancer. Late detection of cancer and the non-organ specific available treatment methods are some of the drawbacks associated with the treatment of cancer. These drawbacks usually lead to the formation of tumours by cancer drugs in unaffected organs as

the drugs used are not organ specific. Researchers have worked hard to come up with a more defined way that can directly target the affected organs in cancer patients, this method encompasses the use of super-paramagnetic iron oxide nanoparticles (SPIONS) as vectors of cancer drugs (11).

A report by the American cancer society shows that about 1688,780 new cancer cases were reported in the year 2017. 35% of these patients were expected to die within 2017; about 11% of these deaths were caused by smoking. Unhealthy lifestyle such as obesity, lack of exercise, alcohol consumption resulted in about 20% of the deaths (15) (16). From the above mentioned statistics from the American cancer society, about 30% of cancer cases can be avoided. The report has also illustrated that about 5 million skin cancer cases are reported annually which may be avoided by protecting the skin from sun exposure by the application of sunscreens (16)

In the developing continents such as Africa, the numbers would be much higher in comparison to America due to the lack of funding in Africa for expensive cancer treatments and detection methods. Therefore, the need for a cost effective method to treat and diagnose cancer in Africa is of importance. Various treatment cancer methods are available such as chemotherapy, immunotherapy, radiation therapy etc. that have been effective in the past but do not specifically target the affected organs thus causing tumours in unaffected organs (15) (17).

The field on nanotechnology has been very robust within the past decades, as it has tried to solve a number of research problems in different fields. Therefore, this study may be a step in the right direction into solving some of the problems associated with drug-targeted delivery in cancer patients.

1.4 Capping agents

The drugs to be administered are usually attached via capping agents to the SPIONS making the capping agent used of great importance; as it determines how much of the drug can be loaded, and the life span. The capping agents may have both negative and positive effects in the properties of the SPIONS such as enhancing the magnetic behaviour, increase or decrease the size, change in morphology etc. Due to the above-mentioned reasons we have formulated a comparison study of three different capping agents i.e. chitosan, PVA and PLGA, evaluating the effect that each capping agent will have on the properties of SPIONS.

The capping agents of choice were chosen due to the fact that they all biocompatible and non-toxic. PLGA is synthesised by poly-condensing two precursors namely lactic and glycolic acid but this method usually yields low molecular weight products. Various modifications within the synthesis would be required to synthesis high molecular weight product should this be the method of choice. One of the modifications includes the use of catalyst such as powdered zinc, Lewis acids etc. PLGA has been identified as a biodegradable polymer thus degrades via normal metabolic pathways within the human body therefore; it was a good choice to use for biomedical applications (12).

PVA is highly biodegradable, nontoxic and is very stable to temperature variation. This polymer is mainly synthesised by the hydrolysis of polyvinyl acetate, the degree of hydrolysis determines the MW, purity of the product of hydrolysis etc. PVA has been used for various applications such as commercial, medical, industrial etc (13).

Out of the three capping agents that were chosen for this work chitosan is the only natural polymer that was used. Chitosan is the product of decylating of chitin, mostly found in the exoskeleton of crustacean animal hence regarded as a natural polymer. This polymer has the ability to chelate with a number of metals due to the amino and hydroxyl groups in its backbone. It is worth mentioning that chitosan is highly biocompatible and is able to biodegrade to normal human body constituents using normal biological cycles. Fibres made from chitosan have been used in various applications such in the production of wound dressing materials, it has be said that materials prepared from this polymer enable accelerated healing as the material is resistant to pancreatic and bile juices attack. Chitosan has also been applied in industry of producing hair care products and pharmaceuticals (14).

The differences in chemical properties present within each capping agent can be the main reason for the differences in the properties of the three-capped SPIONS. Higher molecular weight capping agents may lead to the formation of larger particles; the chemical groups present will also have different affinities for the iron oxide shell thus different interactions. Others may form more stable compounds others less stable due to the different affinities and stabilities associated with each capping agent.

1.5 Research aims and objectives

Aims

The main aims of this study involves the preparation of capped iron oxide nanoparticles using various polymers, this followed by loading the cancer drug curcumin on to the capped drugs and characterising the prepared particles.

Objectives:

1. To synthesise the nanoparticles using co-precipitation route
2. To cap the iron oxide particles using PVA, PLGA and chitosan
3. To bioconjugate the capped particles with curcumin
4. To characterise the SPIONS with various characterization techniques such as HR-TEM for morphological properties, SQUID used for magnetic properties, UV-VIS used to analyse how much of the drug was loaded on to the particles. The crystal structure studies were done using XRD and to analyse for thermal stability of the particles TGA will be used.



Chapter 2

Overview of the chapter

This literature review illuminates some of the characteristics of SPIONS, the various synthetic routes of SPIONS will be enlightened in this chapter namely hydrothermal method, co-precipitation etc.

2.1 Literature review

Iron oxide nanoparticles have been synthesised for use in various applications using different synthetic methods. One of these methods is the preparation of the particles using tannic acid as both the capping agent and reducing agent. This synthetic approach was labelled as a green method of synthesis as it was nontoxic to the environment therefore not producing any by-products that may harm the environment. The main reason behind this was that tannic acid is a polyphenol derivative of plants. This study was aimed at evaluating the antifungal activity of iron oxide nanoparticles on various pathogens such as *Trichothecium roseum*, *Cladosporium herbarum*, *Penicillium chrysogenum*, *Alternaria alternata* and *Aspergillus niger* where different concentrations of the particles were used for this purpose. The particles prepared via this method were characterized using FESEM, TEM and XRD with the antifungal activity evaluated as the inhibition in spore germination as well as by the determination the zone of inhibition.

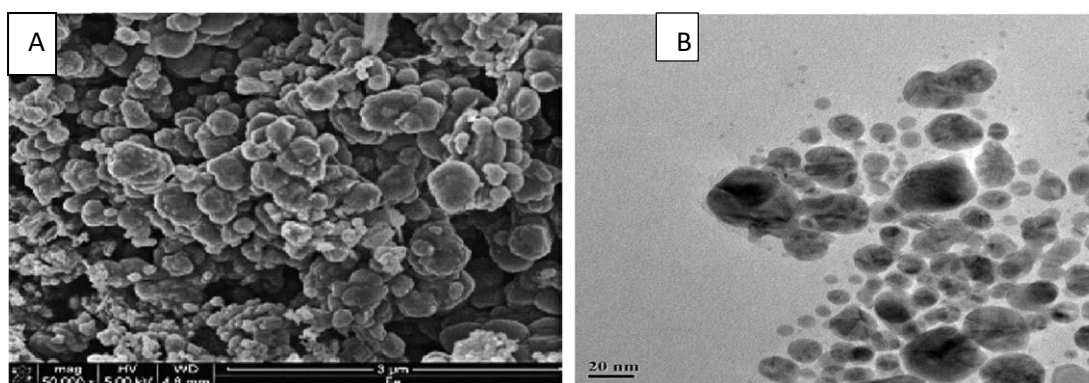


Figure 3: FESEM and TEM micrograph of iron oxide nanoparticles prepared via the green method.

It was concluded from this study that the Fe₂O₃ nanoparticles prepared indicated significant antimycotic activity against all the tested fungal pathogens. Highest inhibition in spore germination was initiated against *T. roseum* (87.74%) followed by *C. herbarum* (84.89%). The highest zone of inhibition by iron oxide nanoparticles was reported against *P. chrysogenum* (28.67 mm) followed by *A. niger* (26.33 mm), *T. roseum* (22.67 mm), *A. alternata* (21.33mm) and least against *C. herbarum* (18.00 mm). Activity index was observed highest against *P. chrysogenum* (0.81). The minimum inhibitory concentration (MIC) value of Fe₂O₃ NP varies between 0.063 and 0.016 mg/ml for different fungal pathogens which is comparable with the standard MIC, revealing the effectiveness of iron oxide NP's against different fungal pathogens (15).

Liu *et al* conducted a study where chitosan capped iron oxide nanoparticles were prepared via the co-precipitation method under magnetic field. SEM, XRD and VSM analytical methods were used to evaluate the change brought about the application of the magnetic field. From this study, it was observed that particles prepared under the magnetic field were rod in shape while those prepared without magnetic field were spherical in shape. This was said to be due to Lorentz force generated from the applied magnetic field. In the presence of magnetic field chitosan capped nanoparticles were said to be assembled along the direction of the magnetic lines resulting in a rod shape (16).

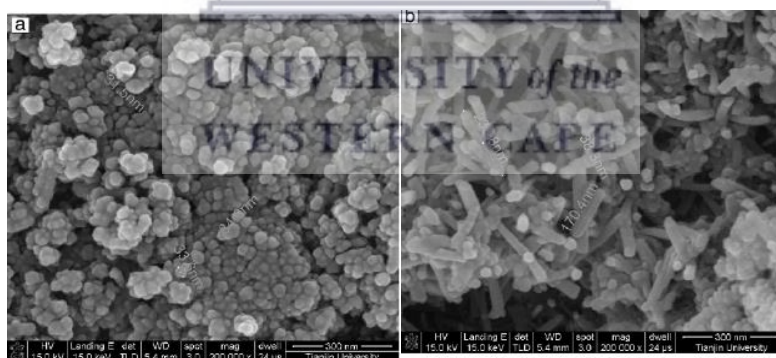


Figure 4: SEM images of (a) iron oxide nanoparticles without magnetic field and (b) with magnetic field

Some of the findings during this study included the increase in the degree of magnetization of the chitosan capped iron oxide nanoparticles in the presence of magnetic field, where without magnetic field magnetization of 13,37 emu/g was achieved this increased to 27,27 emu/g in the presence of magnetic field. Dung *et al* did a similar study where they observe a 15 emu/g saturation magnetization without the presence of the magnetic field.(17) XRD studies indicated various signature peaks of magnetite such as ($2\theta=30, 36, 43, 53, 57, \text{ and } 620$), marked by their indices (220),

(311), (400), (422), (511), and (440)). This was observed for both with and without magnetic field particles, this indicating that the presence of the magnetic field had no effect in the crystal structure and phase of the particles.

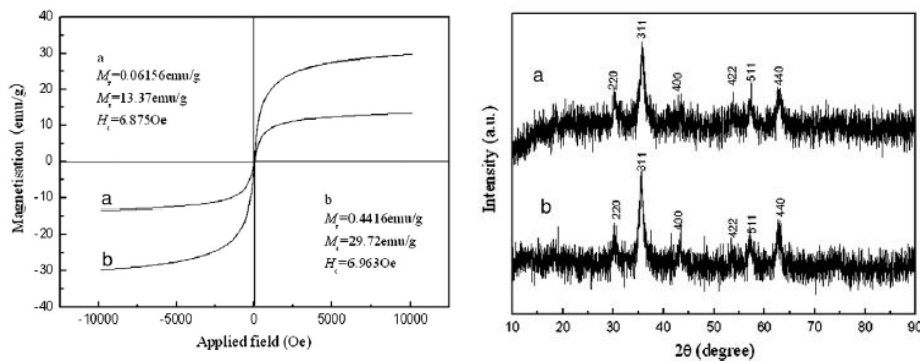


Figure 5: Magnetization curves and XRD patterns of both chitosan capped nanoparticles prepared under magnetic field and without (16).

In another study Fe_2O_3 nanoparticles were coated using Glycyrrhizic acid (GA) extracted from the roots of licorice plant, this was accomplished using the oxidative precipitation route of synthesis. XRD, FESEM, TEM, FTIR, TG, BET were used to characterize the particles.

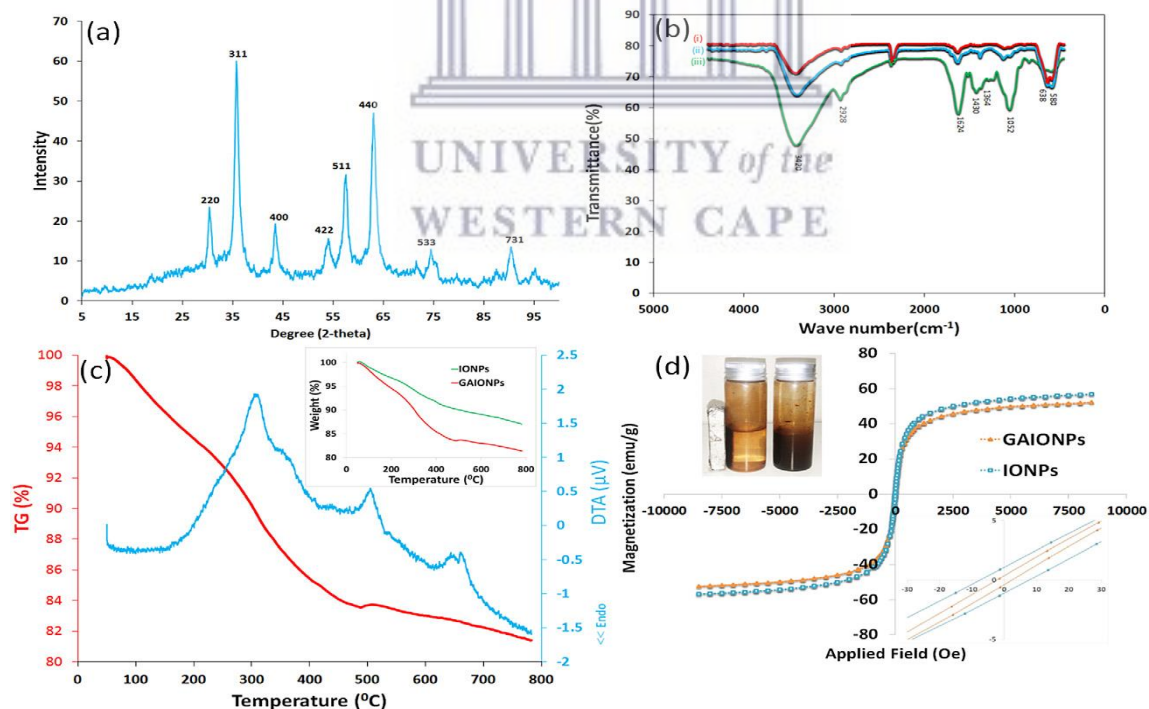


Figure 6: (a) XRD pattern of GAIONPs, (b) Fourier transform infrared spectra of (i) IONPs, (ii) GAIONPs and (iii) GA, (c) TG/DTA analysis for GAIONPs. Inset: TG analysis comparative curves

The data from the study indicated successful synthesis of the iron oxide nanoparticles as well as capping of the particles this proven by both the XRD and FTIR micrographs. The FTIR micrograph depicted in figure 6b indicated the peaks at 1430 and 2928 cm^{-1} , which are related to the bending and stretching vibrations of the C-H bond in the GA respectively. The peak at 1052 cm^{-1} is attributed to the C-O stretching vibration of the GA primary alcoholic functional group. A peak at 1364 cm^{-1} in GA and GAIONPs confirms the presence of carboxyl groups (-COOH). The carboxyl groups are located in both hydrophilic and hydrophobic ends of GA molecule. The carboxyl groups attached to the hydrophobic side were alleged to make hydrogen bonding with the oxygen of Fe_3O_4 whereas the hydrophilic portion is in contact with the surrounding aqueous solution.

It was also observed that the calculated crystalline size of the particles from Debye-Scherrer equation was 18.24 nm while that from the FESEM micrographs was said to be 25.3 nm the difference was said to be from the addition of the capping agent and formation of the agglomerated particles. The study also indicated an increase in the specific surface area of IONPs and GAIONPs measured by BET where the uncapped particles were measured to have 83.569 and 103.936 m^2/g for the capped particles this confirmed the expansion of IONPs specific surface area by GA coating agent making it a more appropriate carrier for drug loading purposes (18)(19).

In a recent study by Seo *et al* (20) SPIONS were prepared via the polyol process which involves the use of an organic medium that will act as both the reducing agent and solvent. ethylene glycol or diethylene glycol are usually the mediums of choice. This method is believed to produce particles with hydrophilic surfaces, high magnetization, as well as the capacity for self-assembly of the synthesized primary nanoparticles into compacted clusters, which can have high magnetization properties. Several parameters determine the quality of IONPs produced during the synthesis such as the type of precursors, reflux temperature, heating rate, reaction atmosphere, as well the surfactants or stabilizers used. NaOH, PVA, PVP and sodium citrate are usually the surfactants used (21). During the study PVP was used as the surfactant whereby the effect of the presence of PVP on the particles was evaluated using various analytical characterization methods such as XRD, TGA and SEM.

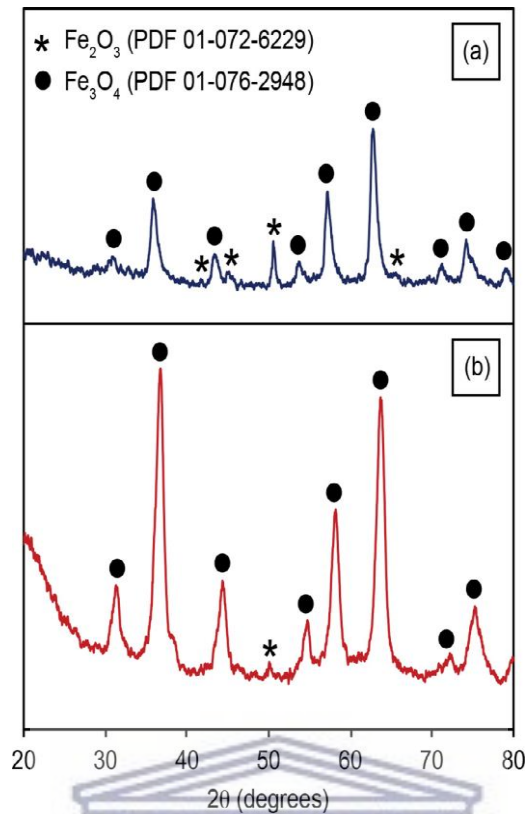


Figure 7: XRD patterns for IONPs (a) without PVP and (b) with PVP

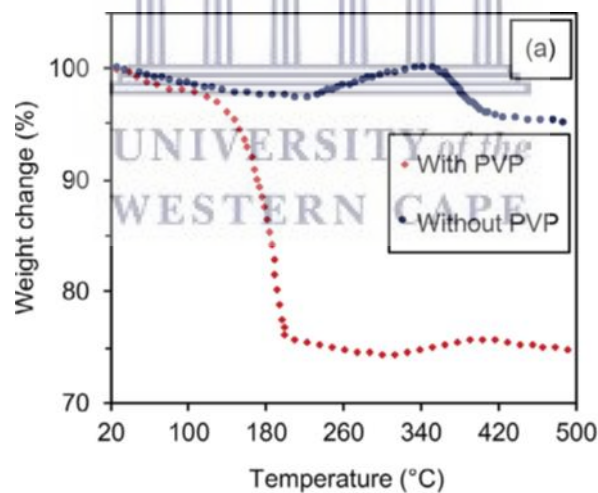


Figure 8: TGA curve of IONPs without PVP and with PVP

Some of the conclusions that were drawn from this study include the decrease in the particle size of the particles whereby the non-PVP particles were 857 nm with the PVP coated particles having size of 225 nm. PVP coated particles were monosized and well dispersed in comparison to the former, this was due to that the non-PVP coated particles were broadly distributed than the PVP coated particles forming large aggregates. Seo *et al* also concluded that PVP protects the nanoparticles from oxidation reaction, as a weight gain was observed in

the PVP coated particles between 320–400°C in contrast to the weight loss experienced over the same period in non-PVP capped particles.

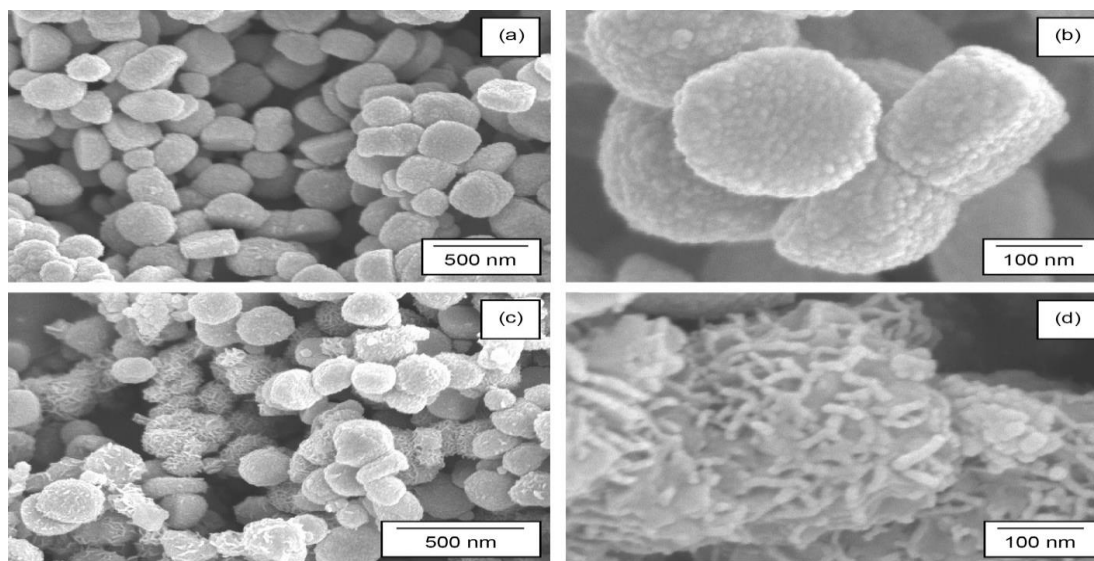


Figure 9: SEM micrographs of IONPs (a & b) without PVP and (c and d) with PVP

From the above SEM micrographs, it was concluded that PVP modified the surface of the particles from dense to porous with chains of iron oxide nanocrystals at the surface of the particle due to steric hindrance. The decrease in particle size proved that PVP might be used to prevent agglomeration of the particles, therefore increasing the surface area opening space for use in various applications such as catalysis (20).

During a study conducted by Burks *et al* iron oxide nanoparticles were investigated for the removal of chromium in water due to its toxicity. The iron oxide nanoparticles were functionalised with 3-Mercaptopropionic acid (3-MPA) which acted as a capping agents adhering to the surface of the particles. The particles were characterised using various methods such as TGA, XRD, TEM and FT-IR. Spherical particles with a mean particles size of 11 ± 3 nm were observed for both the capped and uncapped particles this observed through the TEM images depicted on the figure below. TGA analysis indicated an initial weight loss of 1% for both the capped and uncapped particles until temperature of 200 degrees Celsius this said to be due to removal of water and surface hydroxyl groups. A final weight loss of 3 % and 5,5 % percent were observed for uncapped and capped particles respectively. These losses due to decomposition of amorphous iron hydroxides followed by iron oxide formation for the former while to the loss of surface adsorbed MPA species for the latter. XRD analysis indicated the characteristic peaks are related to (220), (311), (400), (511) and (440) planes of Fe_3O_4 as indexed on the diffraction patterns (22).

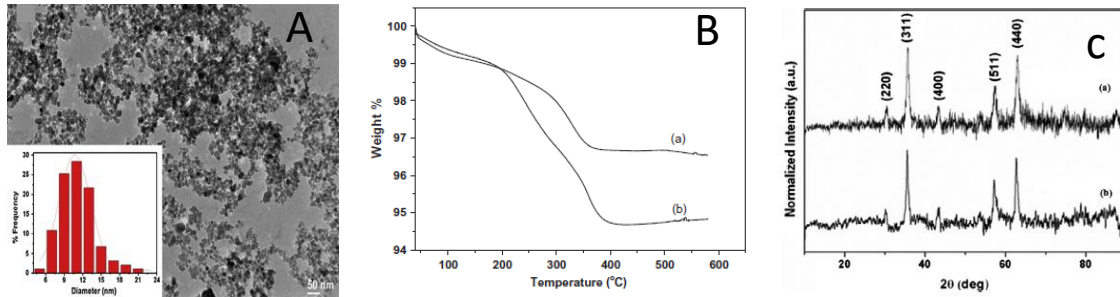


Figure 10: A depiction of the (A) TEM micrograph of capped SPION, (B) TGA curve of a. uncapped SPION, b. capped SPIONS and (C) XRD patterns of the uncapped and capped particles(22)

A study conducted by Paik *et al* involved the study of SPIONS for the development of iron supplements to improve bioavailability of iron in patients suffering from iron deficiency. During this study, surface modified SPIONS with citrate were compared to bare particles. Size distribution studies and zeta potential studies were conducted. The average particle size of the particles from this study were 2078.9 and 219.7 nm for the bare and surface modified particles respectively. To evaluate the zeta potentials of the particles, matrix pH was varied from pH 2 to 12, from this analysis it was concluded that surface modified particles had a lower zeta potential of -35 mV at neutral pH of 7 than of the bare particles of -20 m V. This study also gave a clear indication that surface modified particles were more stable at pH 6 than the bare ones this due to the low surface charge of the bare particles resulting in instability in aqueous matrix. This indicated the presence of citrate in the particles structure might be used to prevent particle agglomeration therefore improving stability of the particles (23).

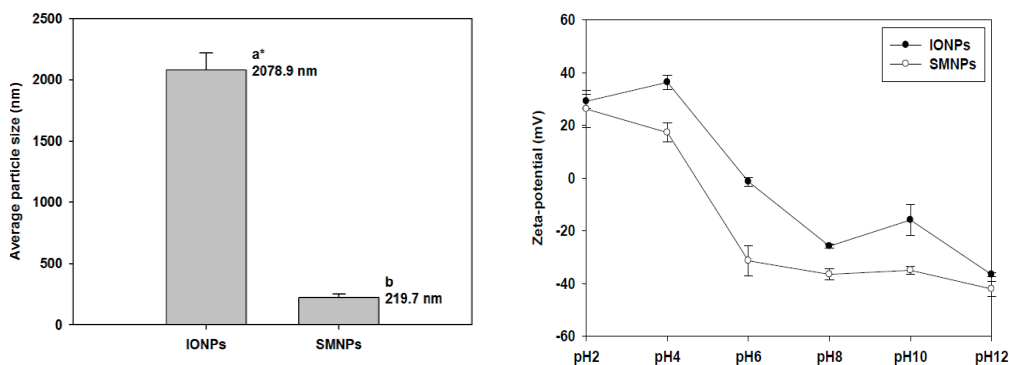


Figure 11: Average particles size and Zeta potential studies of both surface modified and bare particles

2.2 Synthetic routes

Various methods have been utilized to synthesise SPIONs such as microwave, hydrothermal, co-precipitation, sol gel etc. Some of the drawbacks and advantages of the various methods are explained below. When choosing a method of preparation, the environment parameters must be greatly considered as they influence the outcome of the reaction. In industry costs are also of importance, as manufacturers do not want to use an expensive method that will lead to their products being expensive thus minimizing costs is of importance when selecting a synthetic method.

2.2.1 Hydrothermal

This is one of the popular methods of synthesis used to synthesise inorganic nanomaterials due to advantages such as simplistic product morphology control and decent crystallization with high reactant reactivity. The hydrothermal method relies on the use of high pressures and temperatures for the induction or formation of the material. Some of these parameters being the disadvantage of using this method as in other laboratories accomplishing some conditions can be slightly difficult especially if the method is to be used in larger scale (24). The parameters employed have a great impact on the material at hand in addition to these parameters solubility of both reactants and products are also of importance to accomplish the desired product.

Nanomaterials such as nanorods, nanowires, nanotube's, nanospheres etc. have been successfully synthesised using this method. Various researchers have productively synthesised spherical Fe_3O_4 particles with average size of 150-200nm at 90-200°C and quasi-sphere polyhedron nano crystalline Fe_3O_4 with 50nm average size respectively.

When one of the research groups used ferrite and ferric as precursors with NaOH as a precipitating agent in the microwave hydrothermal method, both the iron and precipitating agent were the critical parameters when controlling the products size, shape etc. Fe_3O_4 nano powder has also been previously prepared with ferrite ($\text{FeCl}_2 \cdot 4\text{H}_2\text{O}$) as a precursor and a mixture of NaOH and hydrazine as precipitating agents reacting with ($\text{FeCl}_2 \cdot 4\text{H}_2\text{O}$), with hydrazine seen as the facilitator of oxidation of Fe^{2+} to Fe_3 .

Other researchers have made use of surfactants to synthesise their material where EDTA was used as the surfactant on a reaction between FeCl_3 , $\text{N}_2\text{H}_4 \cdot \text{H}_2\text{O}$ and NaOH controlling both size and shape of the product. To control the shape; Polyvinylpyrrolidone (PVP) with benzene have been used to accomplish different morphologies. Various morphologies such as hexagonal, dodecahedral material were prepared, this done by varying both working conditions and amount of PVP. The work done by various research groups shows that successful attempts have been made in the past to synthesise nanomaterial using this method even with the shortcomings that come with this method as mentioned above(25).

2.2.2 Chemical vapour deposition (CVD) and electro deposition (ECD)

The above-mentioned synthetic methods involve the deposition of precursors onto a substrate to form nanomaterial. For both methods reports are rare due to the shortcomings associated with them such as the need for post-synthesis treatments required to scrape off the material from substrates this limiting their biomedical applications especially in wet chemical environments.

Carbon coated Fe_3O_4 nanoparticles have been successfully synthesised by Rochel *et al* this accomplished by the reduction of Fe_2O_3 using methane and nitrogen in CVD, with carbon used due to its renowned stability and biocompatibility. In another attempt to synthesise Fe_3O_4 via CVD and improve stoichiometry in comparison to when carbonyl is used Mantovan *et al* used $\text{Fe}(\text{C}_6\text{H}_8)(\text{CO})_3$ as a precursor, controlling the thickness of the Fe_3O_4 by CVD pulses.

The difference between the two deposition techniques is that in ECD can be done at room temperature using dissolved ferric or ferrite as precursors. To vary the crystallinity, particles size and orientation changes in deposition potential and electrolyte compositions are usually key to accomplish variation. An ECD method preparing Fe_3O_4 using the same precursors KCH_3COO and $(\text{NH}_4)_2\text{Fe}(\text{SO}_4) \cdot 6\text{H}_2\text{O}$ has also been tried, but varying conditions such as the use of gold-coated polycarbonate as a template, anodic reaction of Fe^{2+} at 80°C under nitrogen environment and preparation on metal substrate respectively. This group of researchers also found a linear relationship between purity of the Fe_3O_4 produced and concentration of acetate in the electrolyte.

2.2.3 High temperature (Thermal) decomposition

The use of low concentrations in other methods of synthesis has resulted in setbacks such as the production of low crystalline material, optimization of particle size and low distribution, as these factors depend on the concentration and rate of reaction of the starting material in low temperature reactions. Therefore, the outcome of those reaction results in limited control over growth and nucleation of the particles (6).

In line for improving the above mentioned setbacks from other synthetic methods; a method to improve these setbacks has been articulated this being the high temperature (thermal) decomposition which relies on extremely high temperatures, which are commonly used to improve crystallinity. High temperatures are not used in other methods such as co-precipitation due to the limiting boiling points of the solvents used in these methods, as some solvents used in other methods have low boiling points.

Literature shows that thermal decomposition of precursors such as Fe (acac)₃ and Fe-oleate in the presence of organic solvents such as benzyl ether, oleic acid, phenyl ether etc which are associated with high boiling points as high as about 300°C, has resulted in successful production of iron oxide nanoparticles with good crystallinity, good size dispersion of around 4-20 nm and controlled shape. The first literature reported by Sun et al where Fe(acac)₃ was thermally decomposed in the presence of organic solvent benzyl ether in order to achieve high temperatures with oleylamine and oleic acid used as surfactants and 1,2-hexadecanediol as the reducing agent of Fe²⁺ to Fe³⁺. The decomposition started at 250°C and finish at around 300°C this indicating that the modification had been successful (26).

This method resulting in well dispersed nanoparticles of size between 4- 16 nm this confirmed using various methods such as XRD, TEM etc. Various research groups have also done work on this method where the method was simplified in such a way as to reduce costs, time and other factors. Some of the changes that have been implemented include using oleylamine as the surfactant, solvent and as the reducing agent, this reducing cost as oleylamine is affordable and resulting in less chemicals being used for the reaction thus less by-products to consider. Another advantage is that oleylamine is known to have weak bonding capabilities with the particles thus can be easily replaced for further modifications of the particles. The nanoparticle size can be controlled by varying reaction time, temperature, as well as solvents with different boiling points.

One of the drawbacks associated with this method is that the particles produced via this method are hydrophobic not hydrophilic as a requirement for applications in biomedicine thus other methods are preferred. Further modifications such as the addition of hydrophilic polymers to particles prepared in this manner may help bring about the hydrophobicity of the particles, such that the particles retain both the properties of the uncapped particles and those of the polymer (3)(25).

2.2.4 Co-precipitation

Co-precipitation method involves the use of an alkaline precipitating agent such as NaOH to precipitate the ferric and ferrous ions in a solvent such as water. This method is the mostly used one from the rest as it results in high product yield, is easy and affordable which is mainly why this method was also used during this study. The iron oxide nanoparticles produced using this method are usually washed with water and ethanol to remove the excess base solution used for the precipitation, the particles produced in this manner are highly rich in OH groups thus aqueous solutions easily suspend them (3).

Many researchers have done work on this method including Refait and Olewe who noted that Fe^{2+} can be used alone in the process if the reaction is conducted under air thus it could produce Fe_3O_4 . They came up with this conclusion after perceiving that they could involve the oxidation of $Fe(OH)_2$ using oxygen in air to produce $FeOOH$ with $Fe(OH)_2$ as an intermediate in the reaction and the precipitation of Fe^{2+} with the precipitated Fe^{2+} and $FeOOH$ reacting to produce Fe_3O_4 (16).

Fe_3O_4 nanoparticles with diameter range of 20 nm- 40nm have been synthesised by varying synthetic parameters this work done by Gao et al where $C_6H_5Na_3O_7 \cdot 2H_2O$, NaOH, $NaNO_3$, $FeSO_4 \cdot 4H_2O$ was used in an aqueous solution, with citrate ions capping the nanoparticles inhibiting aggregation acting as surfactant. Particles prepared on the exterior surface layer of talc mineral by Ah-mad et al were a successful approach where $FeCl_2$ and $FeCl_3$ in NaOH was used for the synthesis in aqueous solution under ultrasonic conditions (3)(27).

2.3 Surface coating

Due to strong magnetic interactions between the magnetic iron oxide nanoparticles, high surface energy and van de Waals interactions the particles tend to agglomerate. This can be inhibited by the modification of the surface of the particles making the shell of the material hydrophilic, various polymers and methods have been used for this purpose. These methods are to be explained in this section.

2.3.1 Au coating

Coating with various metals has been of interest, this due to some of the advantages brought about coating the material with metals as the material retains the properties of the metals leading to the particles having added properties such as protection from low pH corrosion, increased magnetism and so forth. Various metals have been used for this purpose metals such as Zn, copper, Ag, Au etc. Coating with Au has been reported by various research groups with a lot of success, some of the properties that arise when using gold include increased plasmonic properties providing supplementary optic properties and also facilitating organic conjugation by enabling Au-S linkage.

A research group reported the reduction of HAuCl_4 and AgNO_3 at 25°C in the presence of iron oxide nanoparticles synthesised using the thermal decomposition method of $\text{Fe}(\text{acac})_3$ in chloroform producing $\text{Fe}_3\text{O}_4/\text{Au}$ and $\text{Fe}_3\text{O}_4/\text{Au}/\text{Ag}$ respectively, the experimental conditions may vary due to different properties of the SPIONs such as the size, solubility etc. One of the setbacks associated with this method is that of rapid reduction of the Au precursor this leading to the growth of Au nanoparticles instead of the Au capping the iron oxide nanoparticles, this was inhibited by the addition of oleylamine as a slow reducing agent of HAuCl_4 (25).

The research also implied that the use of a strong solvent such as chloroform could facilitate the desorption of the surfactant oleylamine enabling Au growth and nucleation within the shell of the nanoparticles. As the particles still had oleylamine this made them soluble in non-polar solvents thus further drying and addition of sodium citrate and cetyltrimethylammonium bromide (CTAB) was required to make them water soluble, as the adsorption of sodium citrate resulted in making the shell negative, it was also noted that varying the mass of Au and Ag precursors could lead to thicker shells.

In another attempt reduced Au(Ac)₃ with 1,2-hexadecandiol was used in the presence of Fe₃O₄ nanoparticles with oleic acid and oleylamine being the surfactants at 180-190⁰C, with the desorption of the two surfactants facilitated by the high temperatures employed. A centrifuge was used to separate the coated particles from uncoated one as well as separation according to size, as the coated particles would most likely settle at the bottom due to added mass in their structure.

Since the co-precipitation method has been highly used, this aided the synthesis of Au coated nanoparticles with this method this done by sonication of the reactants. One of the setbacks associated with this method was the water solubility and OH groups richness of the surface of the particles. This making the attachment of Au and other metal difficult thus modifications has to be done on the surface of the particles thus attachment of organic linkers such as (3-aminopropyl)triethoxysilane (APTES) which contained amine group that have good affinity for Au³⁺ ions and HNO₃ to make the surface +(ve) charged.

O-benzotriazole-N,N,N',N'-tetramethyluroniumhexafluorophosphate (HBTU) and triethylamine were used as a link between pre-synthesised Au nanoparticles and iron oxide nanoparticles. The covalent bond formed between HBTU and iron oxide nanoparticles was formed via the thiol group of HBTU and Au particles with the product used in the separation of arginine kinase from cell lysate by the application of a magnetic field.

2.3.2 Polymer coating

Due to different properties various polymers have, they have also been used as modifiers of Fe₃O₄ nanoparticles, acting as protective agents as well giving rise to the biocompatibility of nanoparticles. Polymerization of precursors in the presence of pre-synthesised Fe₃O₄ by various methods is the usually synthetic route followed. Below are some of the polymers that have been previously used for this purpose:

2.3.2.1 Chitosan Derivatives

Chitosan as a naturally abundant, biodegradable, less toxic, biocompatible polymer that has been used for various applications such as food processing, biotechnology, pharmaceutical industries etc. In this particular work chitosan was applied for pharmaceutical applications as

a mucoadhesive to achieve controlled drug release. Chitosan is merely synthesised from deacetylating of chitin usually found in exoskeleton of crustaceous water animals (28).

The high density of amino acid groups in chitosan results in the material being a positively charged polymer this aiding in chitosan having good interaction with negatively charged materials such as negatively charged membranes, protein and other polymers, this characteristic leads to it being a good coagulating agent and flocculent.

Chitosan has been reported as chelating material as it is able to bind to proteins, fat's, tumour cells etc, thus the application in pharmaceuticals (drug targeted release in this instance), removal of metals in water such as Cu, Ni and Pb etc.

Due to the difficulty experienced with dissolving chitosan in water and at neutral pH researchers have tried to change this by chemically modifying this polymer resulting in hydrophilic chitosan derivatives (25). To achieve this chitosan was carboxymethylated forming N-carboxymethylchitosan (N-CMC) which is soluble in wide range of pH and has been previously used in orthopaedic devices, connective tissues and achieving controlled drug release. The insolubility of chitosan in water has also been solved by 50% deacetylation of chitin has been proven to be water soluble this was tested when chitosan was to be used in cosmetics as the use of acids could be harmful to human skin or even fatal (29).

Chitosan was used as one of the capping agents investigated during this work, working as a capping agent to the SPIONS produced

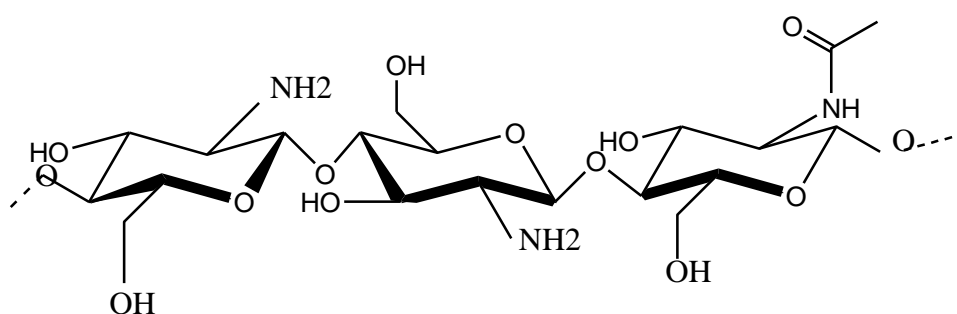
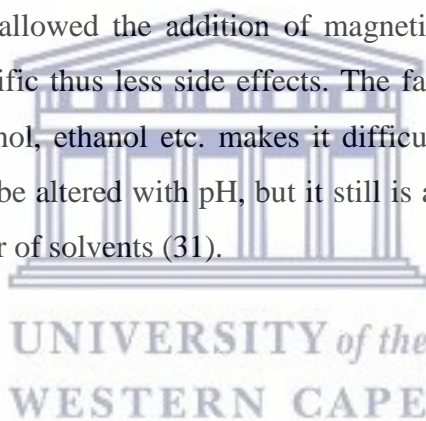


Figure 12: Chemical structure of chitosan (30).

2.3.2.2 Dextran

Dextran a product of fermenting sucrose by *leuconostoc mesenteroides* has been used as carries of macromolecules such as enzymes, drugs, proteins etc. They usually function as hydrogels obtained in either chemical or physical crosslinking depending on the macromolecule being dealt with. Due to the solubility of dextran in water this has led to the use of dextran in carrying various molecules within the body. The conjugation of streptokinase with dextran to treat various conditions such as acute myocardial infarction, acute pulmonary artery thromboembolism, peripheral arterial and deep vein thrombosis has been previously reported. This conjugation reducing cost, increasing the life span of the enzymes within the body and reduced immunogenicity.

The use of dextran has also allowed the addition of magnetic properties thus making the molecules at hand organ specific thus less side effects. The fact that dextran is insoluble in some solvents such as methanol, ethanol etc. makes it difficult to use in other methods of synthesis as solubility cannot be altered with pH, but it still is a good candidate as a capping agent as it is soluble in number of solvents (31).



2.3.2.3 PVA

Polyvinyl alcohol (PVA) the product of polymerization and hydrolysis of vinyl acetate and polyvinyl acetate (PVAc) respectively has been previously used in papermaking, textiles, and a variety of coatings. Both the above preparations steps have been used to tailor make PVA, as the solubility and crystallinity are dependent on the extent of the processes. PVA is soluble in a number of solvents such as Dimethyl Sulfoxide(DMSO), water, Ethylene Glycol (EG), and N-Methyl Pyrrolidone (NMP).

Some of the properties such as the solubility, surface tension and viscosity of PVA merely depend on various conditions such temperature, concentration and molecular weight. Fluctuations in these parameters would affect the degree and character of hydrogen bonding in aqueous solutions. It has been previously reported that highly hydrolysed PVA relates to

low solubility in water. This indicates that one is able to tailor make PVA in this manner as the synthesised PVA would be more liable to use in a specific solvent.

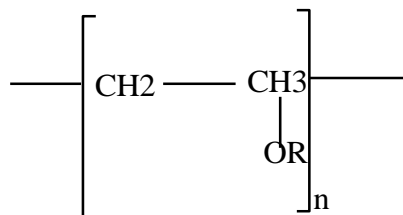


Figure 13: Chemical representation of PVA

2.3.2.4 PLGA

PLGA was used as one of the capping agents during this work to cap SPIONS due to the properties associated with the polymer such as nontoxicity or allergic reactions associated with it when administered in the human body during past research. Various methods have been used to prepare PLGA all of them involving two main precursors namely being poly lactic acid and poly glycolic acid. This polymer is regarded as a biodegradable polymer as it degrades via normal metabolic pathways such as hydrolysis with water where the ester linkage backbone is cleaved to produce monomers. The presence of the alpha carbon in the backbone of this material has resulted in PLGA having two enantiomer Poly-L-lactic acid and Poly-D-lactic acid, with PLGA containing equal amounts of both forms.

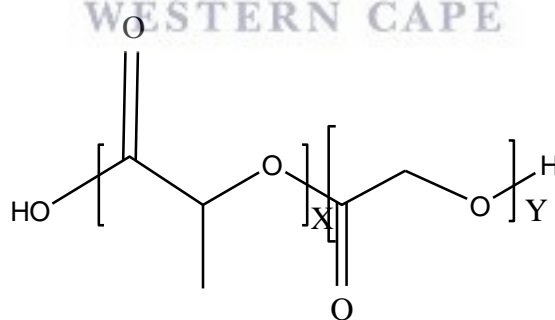


Figure 14: PLGA chemical structure

2.3.3 Carbon coating

Carbon coating is a method, which involves the use of high temperatures as high as 800°C in the carbonization of precursors, it has been used in the past as a method to modify iron oxide nanoparticles. One of the setbacks associated with this method is the reduction of iron oxide

to FeCo. To inhibit the reduction side reaction, pre-synthesised iron oxide nanoparticles were used from the thermal decomposition method. The use of pre-synthesised nanoparticles led to the use of lower temperatures with 365°C highest temperature used.

An example of this work is that of Zhu *et al* where the thermal decomposition method was used to synthesise the uncapped particles. This was followed by the use of an ethylene based photoresist substrate which has been found to have a role in the growth of nerve cell PC12 as the carbon source with the aid of low temperatures. A layer by layer assembly method was utilized where they managed to implant the Fe₃O₄ on to the photoresist silicone substrate followed by the application of low temperature to encourage formation of carbon coated substrate formation leading embedment of the particles with carbon.

During this work, this group noted that there was a linear relationship between the concentration of the Fe₃O₄ particles and the affinity of the substrate to the PC12 cells thus this work can be applied in MRI and hyperthermia studies.

It has been previously reported that particles prepared by thermal decomposition may contain a bit of carbon coating on the surface due to the possible carbonization of precursor used for their preparation. This has been observed when iron oleate is used with docosane as the solvent, this thin carbon layer proved by characterization methods HRTEM and Raman spectra with carbon layers found on both D band and G band of the particles. Carbon coated Fe₃O₄ particles have not proven to be toxic to various cells such as HeLa Kyoto, human osteosarcoma U2OS (GFP-53BP1), NIH 3T3 fibroblasts this in literature said could be due to the thickness of the carbon shell as it may not be thick enough to have contact with the microenvironment.

2.3.4 Drug loading

Due to the non-targeted drug, delivery disadvantage associated with the current chemotherapeutic treatment methods of cancer. Attempts have been made to combat this such as the incorporation of the chemotherapeutic agents within magnetic nanoparticles that will enable targeted drug delivery. Various drugs have been incorporated in the structure of iron oxide nanoparticles this is usually via the capping agent of choice.

2.3.4.1 Curcumin

Curcumin with the chemical structure of bis- α,β -unsaturated β -diketone is regarded as a natural polyphenolic phyconstituent bearing various pharmacological properties. The presence of cyclooxygenase-2 (COX-2), lipoxygenase, and persuadable nitric oxide synthase (iNOS) enzymes has resulted in the recognition of this compound as an anti-inflammatory agent, medicinal therapy for the treatment of various illnesses such as cancer. Due to the low solubility of curcumin, it is likely to be incorporated within highly soluble material in basic solvents. Therefore, it has been incorporated within the highly soluble iron oxide nanoparticles.

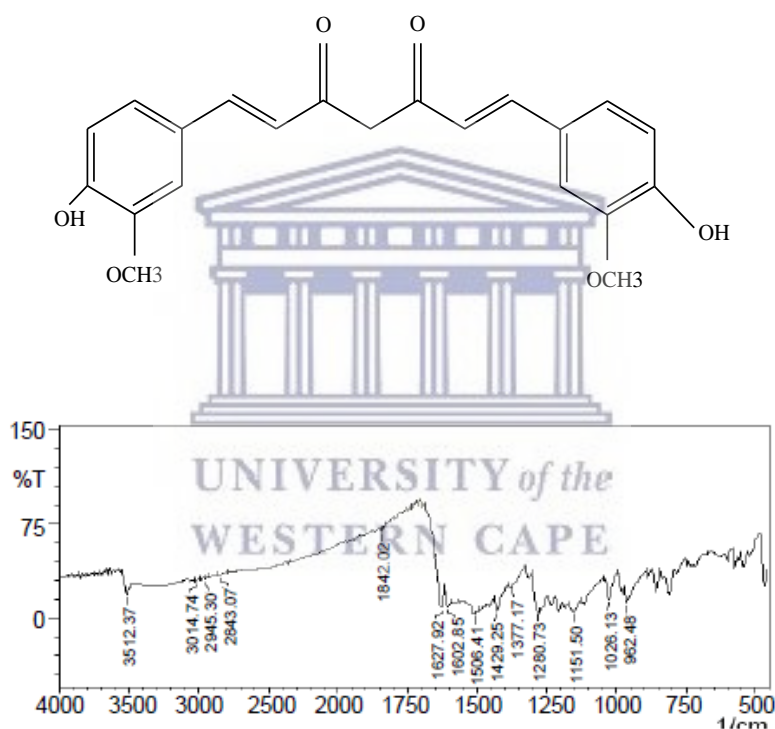


Figure 15: (a) Chemical structure of curcumin and (b) FTIR representation of curcumin

FTIR spectrum of curcumin has a characteristic stretching band of O-H at 3512 cm^{-1} . The peak at 3014 cm^{-1} represents C-H stretching and 1602 cm^{-1} peak was assigned to C=C symmetric aromatic ring stretching. The peak at 1506 cm^{-1} represents C=O, while enol C-O peak was obtained at 1280 cm^{-1} and benzoate trans-C-H vibration was at 962 cm^{-1} . These peaks are credited to the structure on figure 6a.

Chapter 3

Chapter overview

This chapter mainly highlights the methods used to prepare the samples as well as depicting some of the methods used for the analysis of the particles. Various samples were prepared, some prepared in the same way others differently due to the differences in solubility between the polymers used. The uncapped SPIONS were all prepared in the same manner before capping.

3.1 Methodology

3.1.1 Chemicals

Fe_2Cl_3 , Fe_3Cl_2 , Fe_2SO_4 , PVA, PLGA, chitosan, curcumin and ammonia solution were all of analytical grade purchased from sigma Aldrich Company. Solvents deionised water, acetic acid, methanol, DMF and ethanol were used as they are from the laboratory and the characterization was done at different laboratories that are cited in the thesis.

3.1.1 Synthesis

All materials prepared in this work were prepared in the organometallics and nanomaterial's laboratory at the University of the Western Cape.

3.1.2 Uncapped nanoparticles

To prepare the uncapped iron oxide nanoparticles 1,22 g of Fe^{3+} and 1.04 g of Fe^{2+} were dissolved in 60 ML of deionised water in a 3 neck round bottomed flask under a nitrogenous environment. This followed by magnetically stirring the solution at 60°C , followed by the addition of 5 ML NaOH solution drop wise. The solution was stirred (stirring phase) for an hour then washed with deionised water the material collected using magnetic separation followed by drying at 37°C .

3.1.3 Chitosan capped particles

To prepare the chitosan capped particles after the stirring and heating the solution above, a solution containing 0.2 g chitosan, 2 ML acetic acid and 18 ML water was slowly added to this, the stirring and heating continued for a further 30 minutes, the solution separated by magnetic separation, followed by the particles washed with deionised water and dried in an oven.

3.1.4 PVA capped particles

A 20 ML sample containing 20 ML of water and 1g PVA was added to the stirring phase of the bare particles followed by further stirring as above.

3.1.5 PLGA capped particles

PLGA capped nanoparticle were prepared differently from the rest. A 20% solution of PVA was magnetically stirred at 400rpm and heated at 60°C to prepare the surfactant, to the above solution 150 mg of PLGA was added. This was followed by the addition of 4 ML DMF and 100 mg of bare nanoparticles solution was added drop wise forming an oil in water emulsion, the stirring and heating was continued for 2 hours. Then further stirred for 30 minutes to evaporate the organic solvent. Magnetic separation was used to separate the particles from solvent, washed with deionised water and dried using rota vapour.

3.1.6 Drug loading

The same procedure was used to load all the prepared samples with curcumin. For all four samples prepared including the bare batch 30 mg of curcumin and 20 ML of ethanol was sonicated at room temperature this followed by the addition of 10 mg of the of each sample followed by further sonication for 4 hours at room temperature. The particles were then separated using magnetic separation washed with distilled water and dried using rotor vapour then stored for characterization.

3.1 Characterization techniques

3.1.1 FITR

FTIR, which stands for Fourier Transform infrared spectroscopy, is a method of characterization that is mainly used to detect chemical groups present within a sample of interest. This method was used as one of the means to verify successful capping or loading of the capping agents or drug used as they possess different chemical groups to that of the original iron oxide nanoparticles (29).

This method usually works by the application of radiation, which is split into half using a mirror one half of the radiation goes through the sample of interest (which can either be solid or liquid depending on the instrumental design used) the other half is used as reference of the original beam passed. The beam coming from the sample is then compared to the reference beam, the output is then directed to the detector which will show at which wavelengths the sample absorbed radiation this will then give an indication as to which chemical groups are present within the sample as chemical groups absorb at different wavelengths (30).

The samples for analysis were prepared by grinding the samples prepared into powder using a pestle and mortar, then further mixed with KBr, which acted as the background for the analysis.

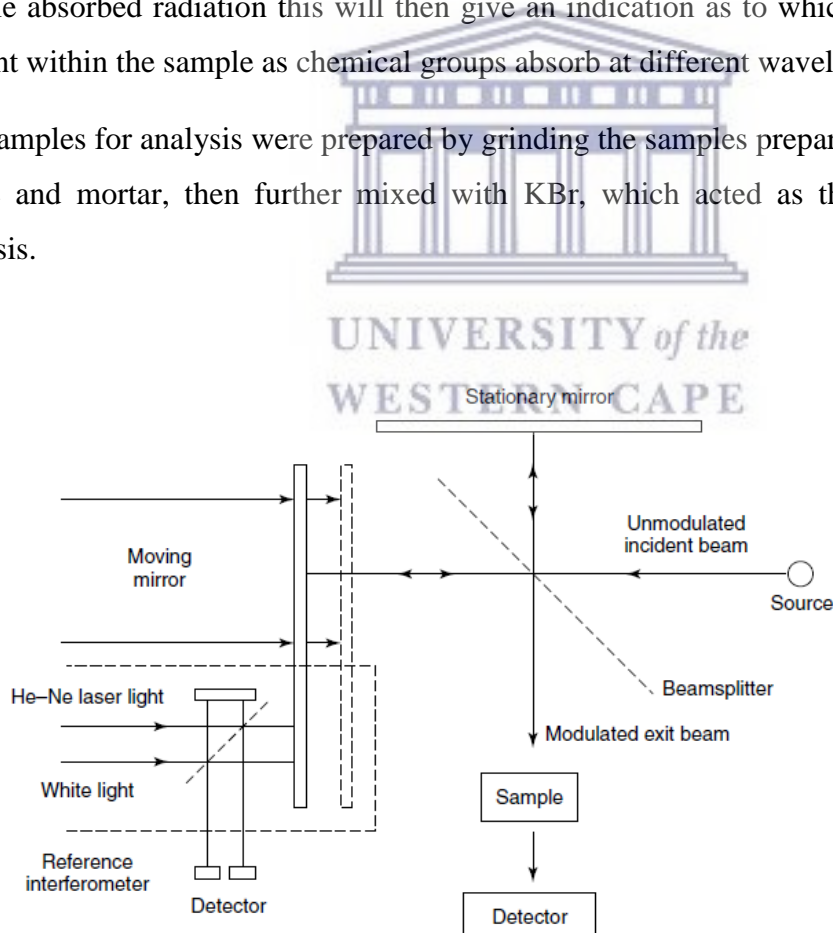


Figure 16: Typical FT-IR setup (32).

3.1.2 XRD

X-ray diffraction (XRD) a method used to determine the orientation of a single crystal, the average spacing's between atoms, can also be used to find the average particle size of material etc , works with respect to brags law $n\lambda = 2d\sin\theta$ thus the representation for XRD is intensity vs 2θ . This information can be used to find the crystal structure of material which can then be used to confirm whether the target compound has been synthesised or not. With all materials that have been analysed using XRD a JCPDS folder is available which will show all the information associated with a specific material with respect to XRD analysis thus when analysing a sample the JCPDS folder is mainly used as a template (33). Newly synthesised compounds may need a new compilation of JCPDS file to have it on record.

The sample to be analysed is exposed to monochromatic x-rays, the beam then interacts with the sample and encounters atoms arranged within the crystal structure, from that encounter the x-rays will then diffract as an output of the encounter as a spectrum with peaks due to x-rays interaction with specific parts of the crystal structure of the sample. A spectrum will then depict the crystal structure this is then compared to all the JCPDS files in the instrument and a final output will be given out by the detector since all compounds diffract the beam differently.

One of the drawbacks associated with XRD is the low detection limit as larger crystalline structure are highly favoured other than small ones, in some instances small ones don't even get detected resulting in skewed results. The advantage of using XRD is that the sample used for the analysis is not lost during the analysis thus it can be used for other analysis techniques which can be good at instances when the product yield is low.

Samples were dried then grinded using pestle and mortar followed by dissolving in specific solvents where required to do so.

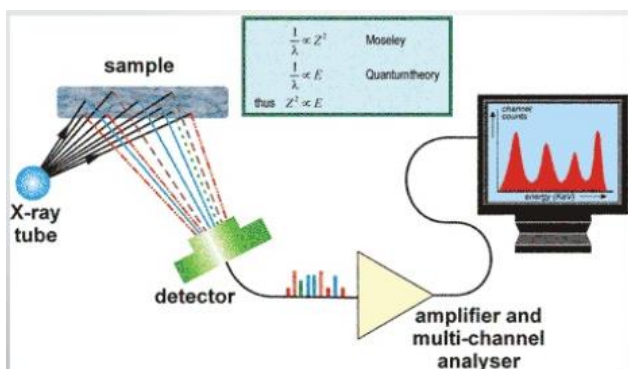


Figure 17: Typical setup of XRD

3.1.3 HRTEM

High-resolution transmission electron microscopy (HRTEM) is a method of analysis that is used to analyse the size and morphology of material. This technique uses the interaction of energetic electrons with the sample and provides morphological, compositional and crystallographic information. The electron emitted from filament passes through the multiple electromagnetic lenses and make contact with the screen where the electrons are converted into light and an image is obtained in a software compatible to the microscope. For the purpose of this work, the prepared particles were dissolved in solvent of choice, placed on copper grid and allowed to dry before analysis.

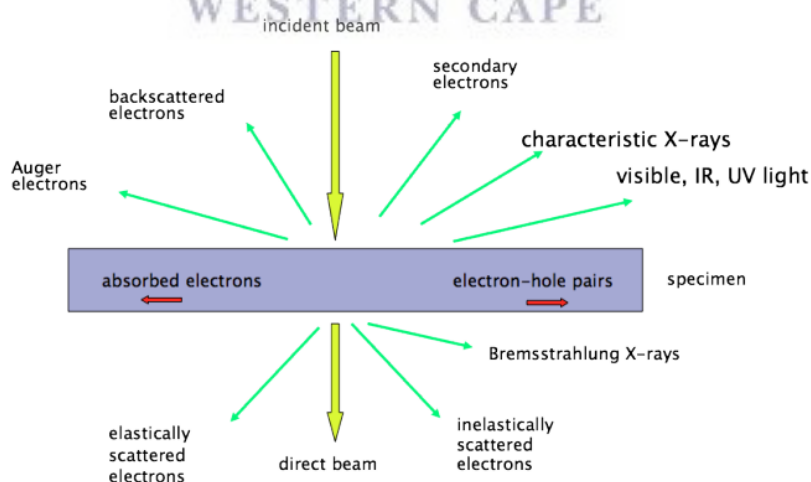


Figure 18: Typical HRTEM interaction with sample (34)

3.1.4 SQUID

Superconducting quantum interference device (SQUID) is an analysis tool used to measure the magnetism of material. This is usually done by the application of a magnetic field on to the sample of interest the device will take note of the saturation magnetization and give it in a plot of magnetization vs magnetic field. This device has the ability of determining whether the material of interest is either paramagnetic or diamagnetic, which can be a tool to determine possible chemical interactions when that material or compound is involved in a reaction (31).

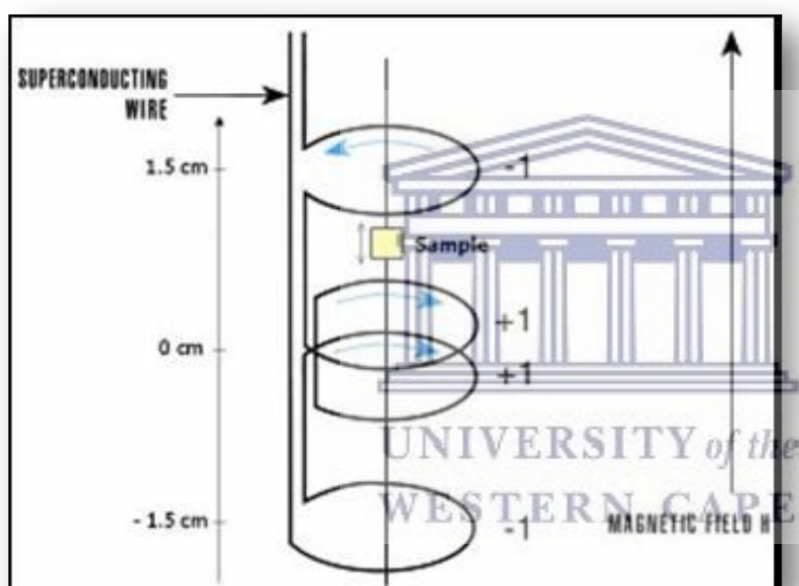


Figure 19: Schematic working of SQUID (31)

3.1.5 TGA

Thermo-gravimetric analysis (TGA) is an analytical method used to monitor weight loss or weight gain as a function of temperature for a given period of time. This is usually done in a temperature controlled facility where all other parameters that may govern the weight loss or gain are kept constant (32). Some compounds may experience a gain or loss of water, oxidise, or decompose due to the application of heat this is then recorded by the TGA decoder system as a curve plot with weight vs temperature as a function of time in other instances as displayed on figure 20. TGA is usually used to determine the thermal and oxidative stability,

decomposition kinetics, life time of materials etc. which change as a function of temperature (33).

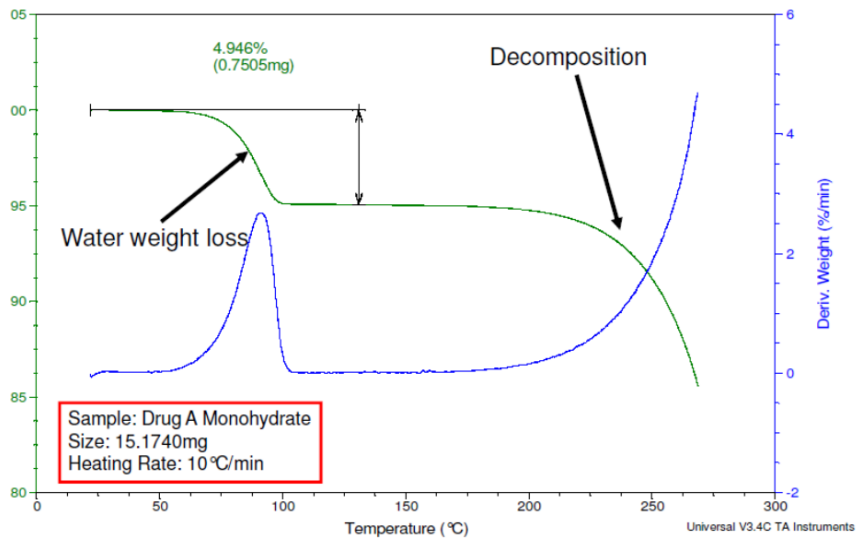


Figure 20: Typical representation of TGA curve (33)



Chapter 4

Chapter overview

This chapter mainly illustrates the results of this project as well as tries to make sense of these findings. Results from all the characterization techniques engaged during the course of the project are depicted in this chapter in the form of tables and figures.

4.1 Results and discussion

4.1.1 HRTEM

Micro graphed below is the HRTEM images, HRTEM is a spectroscopic analytical instrument used for the determination of particle size and shape. Depicted below at Figure 21 and 23 are HRTEM images of the prepared particles. Figure 22 and 24 depict the particle size distribution of the particles.

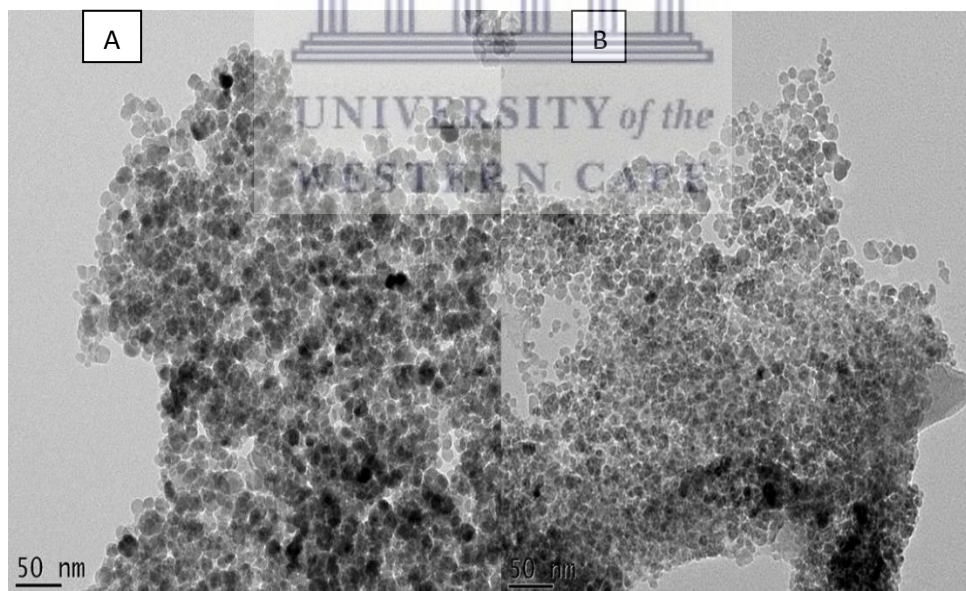


Figure 21: (a) Uncapped SPION nanoparticles (b) chitosan capped SPION particles

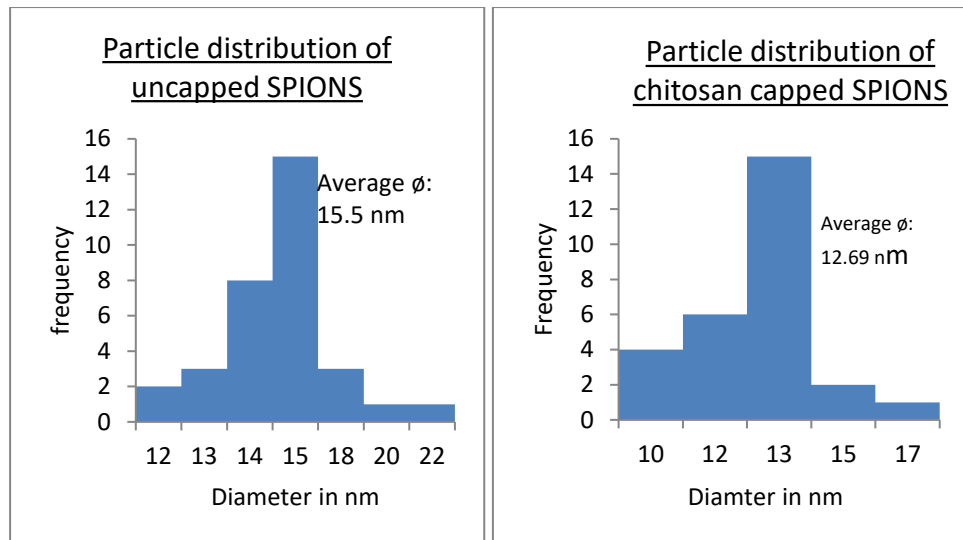


Figure 22: Particle distribution histograms of (a) uncapped SPIONS and (b) chitosan capped SPIONS

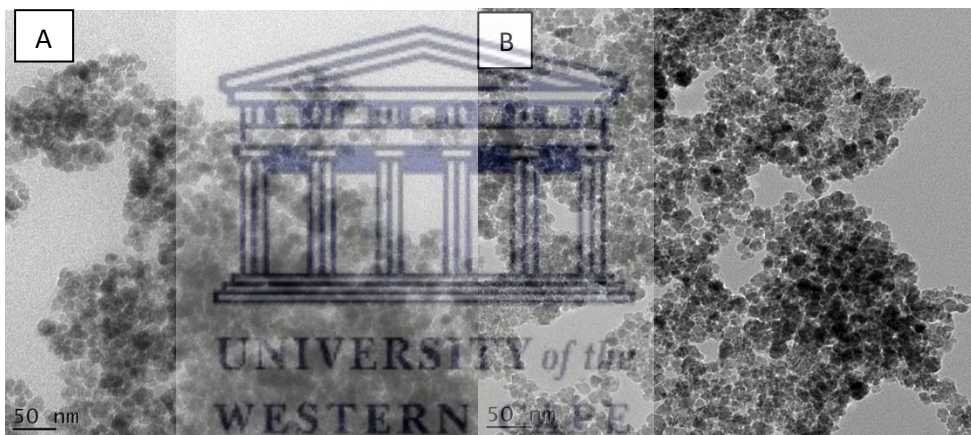


Figure 23: (a) PLGA capped SPION nanoparticles (b) PVA capped SPION nanoparticles

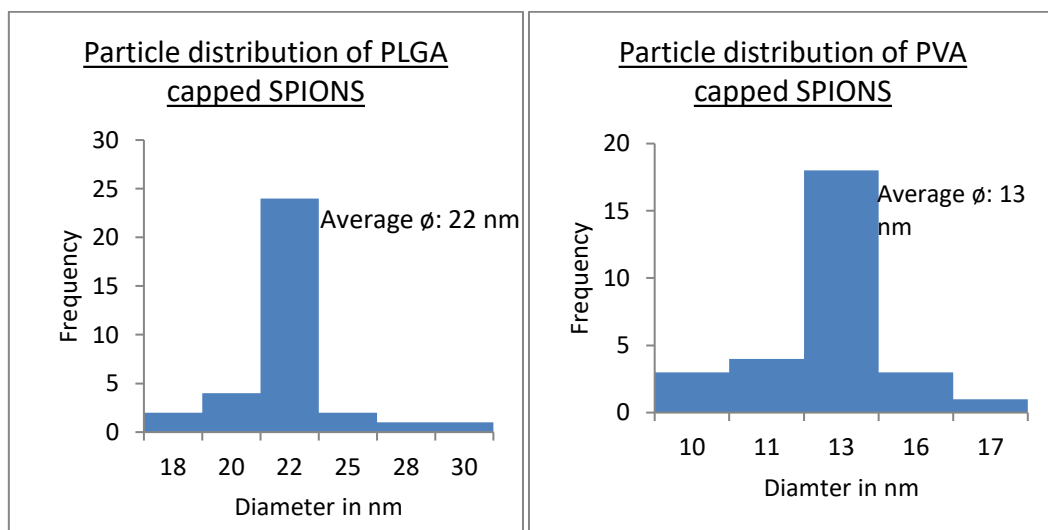


Figure 24: Particle size distribution of PVA capped SPIONS

HR-TEM micrographs were taken for both the uncapped particles and the capped particles with various capping agents. It can be seen from the micrographs that all the particles are spherical in shape, which has been seen as the most prominent shape prepared from the co-precipitation method. The spherical shaped particles have been observed in other published work from Liu *et al* where the particles prepared without a magnetic field as in this work were spherical in shape and that of particles prepared under a magnetic field were rod in shape (16).

SPIONS are mainly composed of iron and oxygen molecules, which react in a dipole-to-dipole manner therefore agglomerating. In our work, bare SPIONS show a higher degree of agglomeration than the capped particles this depicted on the images above as expected. In some of the micrographs, the degree of inhibition of agglomeration is slightly observed where capping agents are used. The low degree of inhibition may be eliminated by the increase in concentration of capping agents used as well as sonicating SPIONS during preparation for increased reaction times. The low degree of inhibition can be due to the short reaction time therefore the reaction requiring prolonged times to allow the inhibition process. The reaction times may also have been long thus resulting in the amputation of the capping agent from the SPIONS over prolonged reaction times as the samples were agitated. Particles capped with chitosan were observed to have a higher degree of inhibition than the PLGA capped ones seemingly as the least initiator for inhibition of agglomeration.

HRTEM images in conjunction with Image J software were used as a method of evaluating average diameters of the SPIONS. From the above results it may be noted that PLGA capped particles had the highest particles size of 22 nm average than the other SPIONS. The chitosan and PVA capped particles had almost the same diameter of 12.69 and 13 nm respectively. During a study conducted by Zeinali *et al* chitosan capped SPIONS averaged at 13.5, 9.6 and 7.7 nm were accomplished, during the work sonication times were varied with an increase in the sonication time resulting in smaller sized particles. This was reasoned by the fact that prolonged sonication times resulted in higher degree of agglomeration. Since this group of researchers got about 13 nm with 30 min sonication during the preparation of their particles in comparison to the 12.69 nm from this work without any form of sonication should be indication that the method of preparation used for this work may be more efficient than the former (35).

4.1.2 FTIR

The functional groups in a compound act as the DNA fingerprint of that specific compound. This can be identified by versatile equipment referred to as the FTIR. Below are the FTIR micrographs for all the synthesised particles. This analysis was used to determine whether the designated materials were successfully prepared by the method of choice, this will be distinguished by the presence of various chemical groups present within each compound added to the particles. Figure 20 is a depiction of the uncapped-unloaded particles and the loaded with curcumin particles. The capped particles FTIR micrographs are portrayed in figure 26.

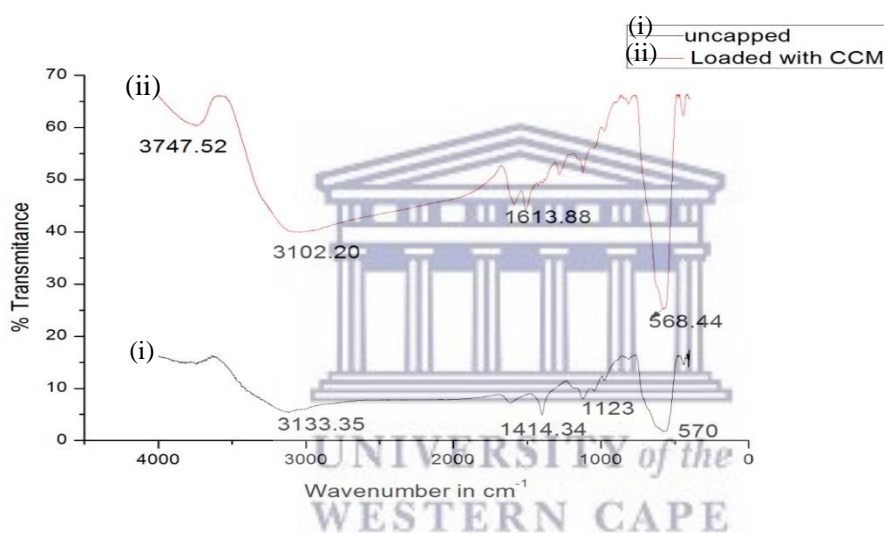


Figure 25: Fourier transform spectrum of uncapped and loaded particles with CCM

The Figure 25 above is the Fourier transform representation of the uncapped as well as loaded iron oxide nanoparticles, the successful synthesis of the particles may be determined by the following peaks, which are signature peaks for iron oxide nanoparticles. The formation of the highly intense Fe-O stretching at 570 cm^{-1} , with high intensity indicates a high occurrence of this bond within the crystal structure of the nanoparticles. Various signature peaks of curcumin were observed for figure 25 above. The 3450 cm^{-1} peak representing C-H stretching with the 1580 cm^{-1} assigned to C=C symmetric aromatic ring stretching as depicted by figure 11 in chapter 2. The highly intense peak at 3451 cm^{-1} illustrates the characteristic stretching of the O-H band associated with curcumin. Jian-Min et al found the character peak at 590 nm illustrating the presence of Fe_3O_4 can be said to be the same peak found during this research between 560 nm- 580 nm in all the particles prepared (36). However, this helped to confirm the successful preparation of the base compound SPIONS.

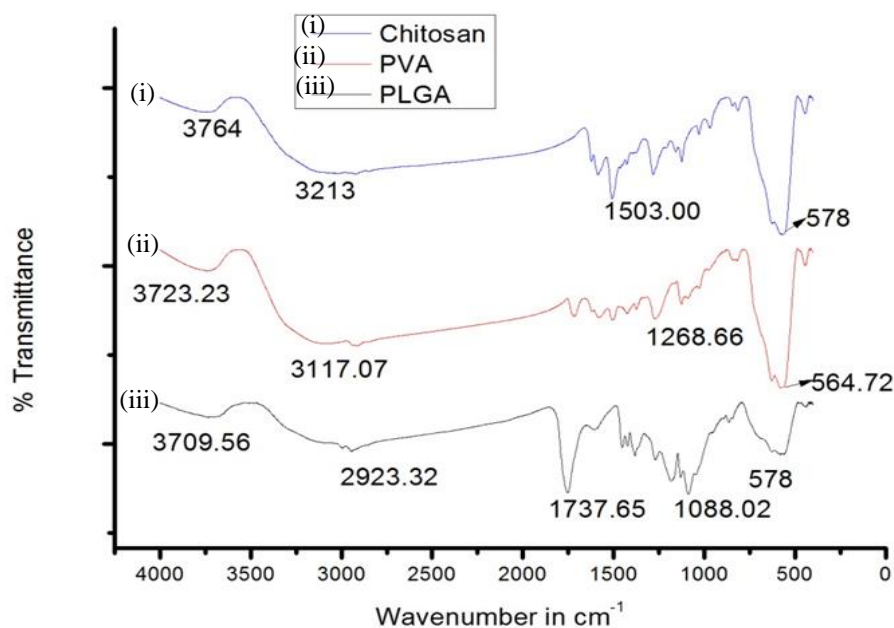


Figure 26: Capped and loaded with curcumin SPIONS

The successful capping of the SPIONS is evident from Figure 26 because of evident changes in the functional detected from the uncapped sample to the capped ones. It is evident that the O-H stretching observed in Figure 25 of the uncapped-unloaded SPIONS the band has slightly changed when comparing with the loaded and capped SPIONS. Jian-Min *et al* also prepared PLGA capped particles iron oxide nanoparticles and found the C-O stretching band at 1060 nm indicating the presence of PLGA. We similarly observed on the FTIR spectra during this work that the same peak situated at 1088 nm which confirmed that PLGA was encapsulated within the particles (36).

In the PVA capped samples the high OH content of the molecule may be depicted by the distinctive broad peak at 3117 cm⁻¹. Other changes such as the appearance of various intense peaks around 1093 cm⁻¹ are indicators of changes within the structure of the bare particles in comparison to the capped particle this band indicating the presence of C=O and C-O stretches from the remaining acetate groups in PVA.

4.1.3 Zeta potential

Zeta potential measurement is the measure of the electrical charge of particles suspended in a solvent of choice. This analysis was conducted during this work to analyse for any changes in

the charge of the particles before and after capping the particles with the capping agents. Figure 27 depicts the charge on uncapped particles as well as charge on capped particles.

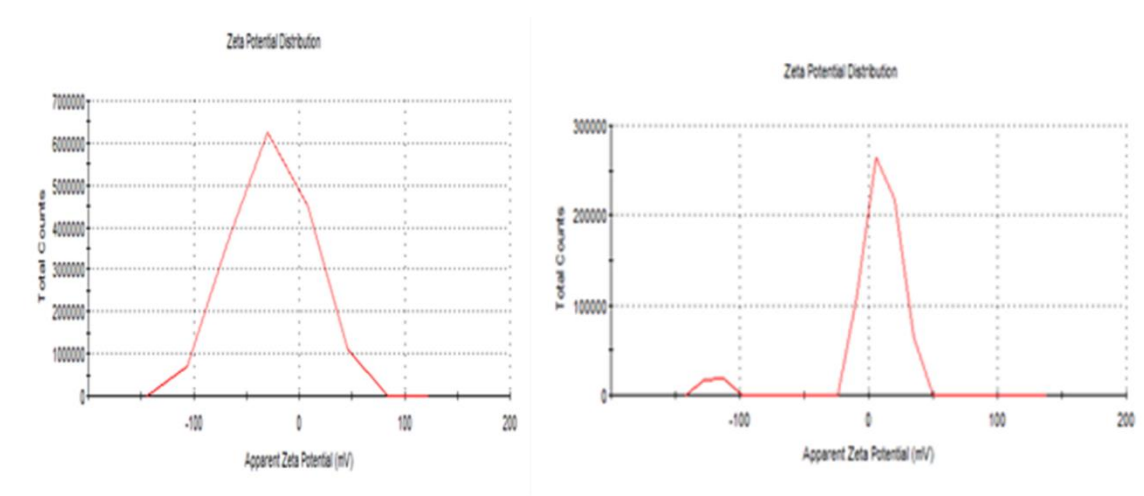


Figure 27: Zeta potential of bare material and Zeta potential of capped nanoparticles

From the above figures, successful capping of the particles has been clearly depicted, as a change in the charge has been knowledgeable. Figure 27 showing the charge of bare material at -37 mV and Figure 27 where capping has been done with a polymer being about 6mV this proving successful capping of the particles. The PVA and chitosan showed these characteristics but with PLGA, this was not detected as it was difficult to do the analysis due to the corrosion of the cuvettes by the solvent used. Paik *et al* prepared surface modified nanoparticles and found that at pH 6 the surface modified particles were more stable than the unmodified particle's, this was the opposite at lower pH values. In this study, the capped particles were found to be less stable than the uncapped but the pH was not varied due to time constraints (23). Therefore, a further study to evaluate the effect of different pH values on the stability of the capped particles is required as this would give more insight to the stability of the particles and determine whether they may be used within the human body.

4.1.4 XRD results

XRD is a method of analysis used for the determination of the crystal structure of particles; this information is used to determine the particle size in conjunction with Debye-Sherrer equation. Illustrated in figure 24 are the XRD plots of the uncapped SPIONS, PLGA capped, PVA capped and chitosan capped SPIONS. Tabulated on table 1 are the particle size of all the particles determined by the Debye-Sherrer equation.

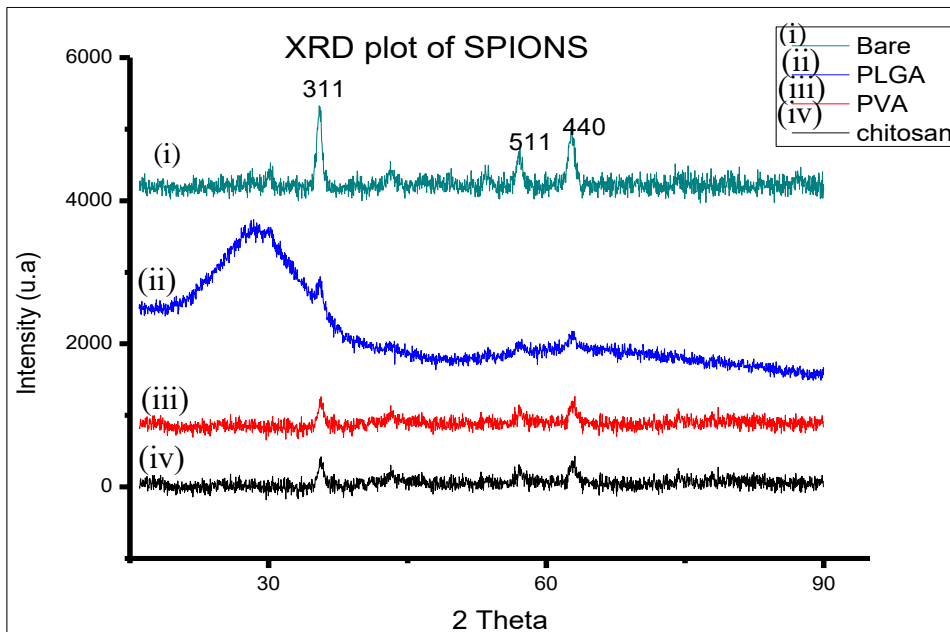


Figure 28: X-ray diffraction representation of various SPIONS.

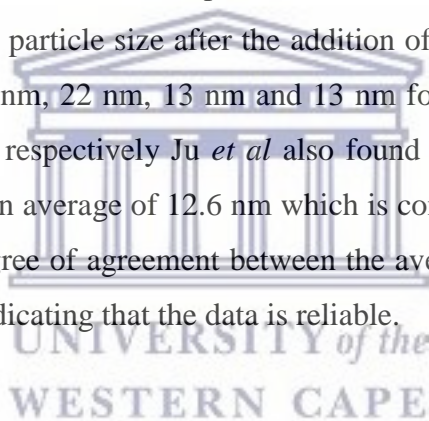
Table 1: Determination of particle size by Scherer equation

Sample	2 Theta	Theta	Cos Theta	Radians	FWHM	Wavelength	Beta	Radians	d(311) in nm
Bare	35,4643	17,73215	0,9524	0,309603	1,0282	0,154	0,5141	0,008976	14,54999
PLGA	35,5638	17,7819	0,9522	0,310472	0,6634	0,154	0,3317	0,005791	22,54621
PVA	35,592	17,796	0,9521	0,310718	1,07794	0,154	0,53897	0,00941	13,87423
Chitosan	35,6302	17,8151	0,952	0,311052	1,07793	0,154	0,538965	0,00941	13,8729

XRD analysis was used to obtain the particle size and crystal structure of both the capped and uncapped SPIONS. Figure 28 above depicts an inverse spinel assembly for all the capped particles and uncapped. A slight change in the assembly of PLGA particles was observed this could be due to the problems encountered while drying the sample. Various methods were attempted such as the oven drying, freeze-drying and rota vapour drying which did not really prove to be hundred percent successful, thus there could have been moisture within the sample, altering the structure of the particles. The signature peaks associated with magnetite were observed within the XRD plots namely (220), (311), (400), (422), (511), and (440). This work can be compared to that done by Jian-Min *et al* also found the exact peaks from the work conducted. It can be concluded from the micrographs that the presence of additional matrix brought about the addition of polymers to the structure resulted in the reduction of the

intensity of the peaks this was also the case from the work conducted by Shen *et al* (36). During the preparation of chitosan capped iron oxide nanoparticles by Liu *et al* the same character peaks were observed regardless of the presence of magnetic field as well as the presence of chitosan. This indicating that the presence of the magnetic field and the capping agent did not alter the phase of the iron oxide nanoparticles; this was the case for this work, as the presence of the capping agents did not change the phase of the particles (16).

The most intense peak indexed at (311) in all the particles was used as an estimate of the particle size with relation to the Sherrer equation ($d(311) = k\lambda/\beta\cos\theta$) (3). The particle sizes have been displayed on Table 1 above. From the data above it can be noted that the particle size tends to decrease after the addition of capping agents except in the case of PLGA which had problems during the synthesis thus further investigations and synthesis is required. Pardoe *et al* also observed the decrease in size after the addition of a capping agent. Where they also prepared PVA capped particles and compared them with dextran capped particles experiencing a decrease in the particle size after the addition of the capping agents (37). The particle sizes ranged from 14 nm, 22 nm, 13 nm and 13 nm for the uncapped, PLGA, PVA and chitosan capped particles respectively Ju *et al* also found similar sized particles during their work where they found an average of 12.6 nm which is comparable to the results of this work (1). There is a high degree of agreement between the average particle sizes from both the HRTEM and XRD data indicating that the data is reliable.



4.1.5 SQUID

SQUID is an analytical method used for the measurement of the degree magnetism of a material; the magnetism is displayed as a hysteresis curve, which may also be used to estimate the coercivity of a material. Displayed below is the hysteresis curves of the uncapped, chitosan capped, PVA capped, PLGA capped as well as that of uncapped curcumin loaded iron oxide nanoparticles.

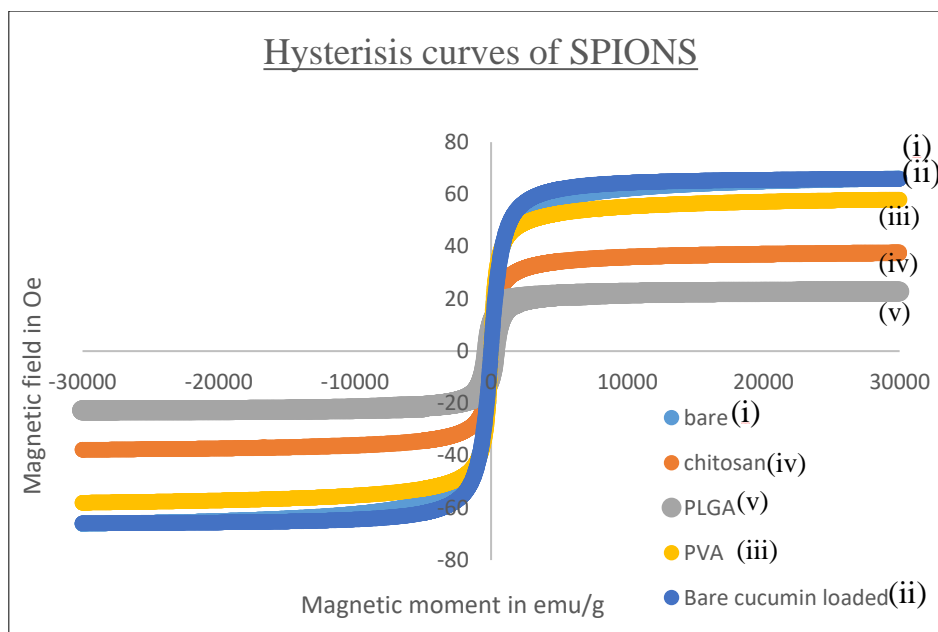


Figure 29: Depiction of magnetism of the particles

From the above results the uncapped particles contained a saturation magnetization of 70 emu/g at maximum applied magnetic field of 30000Oe this was in agreement with the results from Dung *et al* who also prepared uncapped iron oxide nanoparticles, while Osuna *et all* had that of 73,2 emu/g.(38)(17) It may also be highlighted that the value from this work was higher than that of a similar study by Ling *et al* of 60emu/g (39). This gives an indication that the particles were successfully synthesised as the value obtained in this work is in agreement to that of most literature studies if not better.

The same value was found for curcumin loaded particles this might either indicate that the addition of this drug had no effect in the magnetism of the particles. The drug may have been unsuccessfully incorporated onto the structure or very little of it may have been present thus insignificant change in the magnetization. The unsuccessful incorporation of curcumin may be due to the absence a polymer which are mostly used to assist in the attachment of the drugs onto the material. From the results it can also be noted that there is no coercivity in all the particles prepared via the co-precipitation method from this work as all the curves intersect the graph at zero horizontal intercept.

The results above also indicate a saturation magnetization of 30emu/g for chitosan capped particles which is higher than that of Dung *et al* of 15emu/g but lower than that of Osuna *et all* of a very high 65,6 emu/g (17)(38). This high saturation magnetization of Osuna *et all* may be attributed to the very low content of chitosan used as the title of their work also indicated that very low concentration of chitosan was used for their work. The PLGA capped

particles had a much lower magnetization saturation than the rest of the other polymers used for the capping of the particles of 23emu/g which is a bit lower than that from Shen *et all* of 27emu/g where they also incorporated the drug doxorubicin and verapamil (36). This lower value may be attributed to the increased thickness of the shell as two polymers that were “utilized” for the capping of these particles, as PVA was used as a surfactant for the encapsulation of PLGA onto the nanoparticles hence an increased shell thickness lowering the magnetism of the particles.

PVA capped SPIONS showed a very much lower percentage reduction of the saturation magnetism from the uncapped particles as the particles obtained a saturation magnetization of 58emu/g, which is a 17% reduction of the magnetism experienced from the capping of the particles. Bolden *et al* had a very much lower saturation than that from this work as they had about 31,32emu/g at the same temperature of 300K (40).

4.1.6 TGA

Thermo-gravimetric analysis (TGA) shows the variation in mass with increase of temperature. Below are the Thermo-gravimetric curves of the prepared SPIONS.

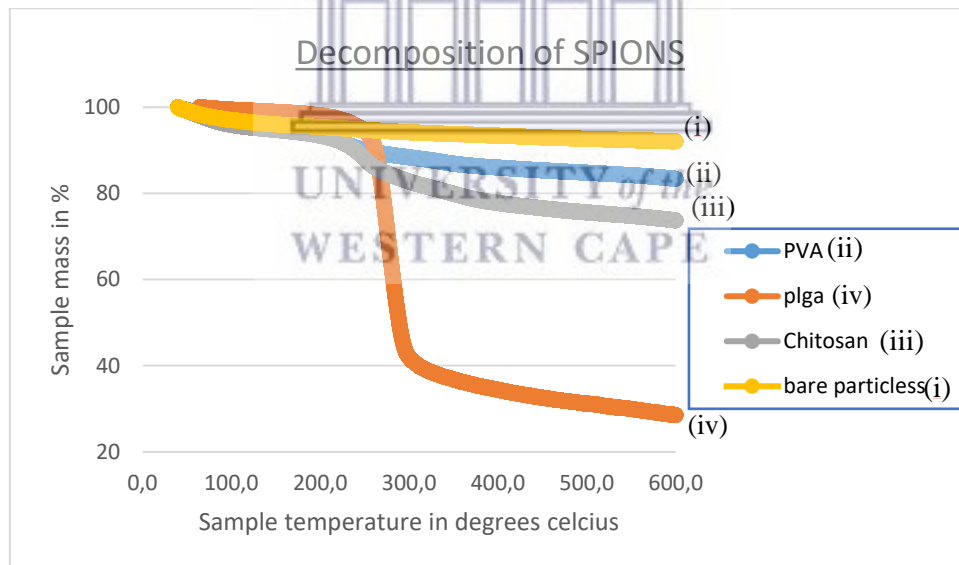
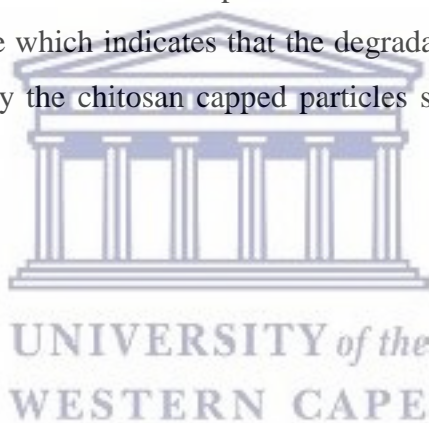


Figure 30: TGA curve of SPIONS depicting the decomposition of the particles

Figured below are the ther-mograms of the prepared SPIONS using the co-precipitation method. All the particles primarily experience a decrease in mass of about 5% if not less, this loss is attributed to the removal of surface hydroxyl and water. Uncapped particles having an overall loss of 7,3% which is the lowest loss of mass experienced from the study. PLGA particles experienced the highest loss in mass of 73% at 290°C, this high decrease in mass

may be due to the melting point of PLGA is 280°C hence this high loss of mass at that temperature. This indicates that most of the PLGA capping agent was lost during this period. This observation may also be used as an indication of the successful incorporation of PLGA on to the SPIONS surface. Burks *et al* which did a relevant study primarily experienced a loss of 1% for both the capped and bare particles, followed by a further loss of 3% for the bare particles this loss in mass is lower than the loss experienced during this work (22). The amplified mass loss during this study may be attributed to the high initial mass used during the analysis.

Chitosan capped particles had a loss of 28% this occurring from 210°C- 600°C, this is the second highest loss between the capped particles. Catalano *et al* also experienced degradation of chitosan capped particles from 210°C- 600°C this was further followed by weight gain at higher temperatures. During the study the maximum used temperature for the analysis was 600°C hence the increase in mass was not experienced. The reported results above are in agreement with most literature which indicates that the degradation temperature for chitosan is 220°C which is merely why the chitosan capped particles start degrading at around that temperature (41).



Chapter 5

5.1 Conclusion

In conclusion, the objectives of this work were achieved as the PLGA, PVA and chitosan capped SPIONS were successfully synthesised using the co-precipitation method. The success of this work is confirmed by the methods XRD, SQUID, FTIR and TGA. These analytical methods have clearly depicted the incorporation of the capping agents. With the inverse spinel structure shown by XRD analysis, as it is a signature depiction of magnetite.

From the XRD analysis, it may be noted that the PVA and chitosan particles bring some sort of restriction to the size of the particles when compared to PLGA. This study has indicated that the PLGA polymer might be the preferred of the three evaluated where larger particles are required, as this polymer does not restrict the size of the particles but requiring a good drying method. This study also indicated that the presence of the capping agents has the ability to reduce the saturation magnetization of the particles depending on the polymer of choice but with PLGA in this instance having the higher reduction this shown by the SQUID results. Where higher saturation magnetization is a requirement for applications PVA capped particles will be the best choice. TGA analysis indicated that all the particles start decomposing at 200 degrees Celsius with PLGA losing the most amount of mass during the interval of 200-600 degrees Celsius. From the three polymers used from this work it is not very clear which one is the best as all three have strong points in different analysis. Therefore, it is recommended when choosing a polymer, it is essential to highlight what properties would be valuable for the particular application.

5.2 Future work

Some of my future work involves the:

- Preparation of PLGA capped SPIONS with a different drying method
- The variation of concentrations for the capping agents and that of drug
- Assessment of the reaction times to verify good inhibition of agglomeration period
- As well as the variation of matrix pH to evaluate zeta potential

5.3 References

1. Hu J, Hu X, Chen A, Zhao S. Directly aqueous synthesis of well-dispersed superparamagnetic Fe₃O₄ nanoparticles using ionic liquid-assisted co-precipitation method. *J Alloys Compd.* 2014;603:1–6.
2. Wu S, Sun A, Zhai F, Wang J, Xu W, Zhang Q. Fe₃O₄ magnetic nanoparticles synthesis from tailings by ultrasonic chemical co-precipitation. *Mater Lett* . 2011;65(12):1882–4.
3. Indira T. Magnetic Nanoparticles: A Review. *Int J Pharm.* 2010;3(3):1035–42.
4. Sun S-N, Wei C, Zhu Z-Z, Hou Y-L, Venkatraman SS, Xu Z-C. Magnetic iron oxide nanoparticles: Synthesis and surface coating techniques for biomedical applications. *Chinese Phys B.* 2014;23(3):037503.
5. Gribouski E, Jaimes R, Sotak C. The Use of Iron-oxide Nanoparticles for Hyperthermia Cancer Treatment and Simultaneous MRI Monitoring A Major Qualifying Project Submitted to the Faculty of In partial fulfillment of the requirements for the Degree of Bachelors of Science in Biomedical En. 2009;
6. Manuscript A, Sun C, Du K, Fang C, Bhattarai N, Veisoh O, et al. NIH Public Access. October. 2011;27(9):2528–43.
7. Qiu D, An X, Chen Z, Ma X. Microstructure study of liposomes decorated by hydrophobic magnetic nanoparticles. *Chem Phys Lipids.* 2012;165(5):563–70.
8. Vashist SK. Magnetic Nanoparticles-Based Biomedical and Bioanalytical Applications. *J Nanomed Nanotechnol.* 2013;04(02):2.
9. Fe MOM. Synthesis and Characterization of Magnetic Nanoparticles of the. 4:1–13.
10. Sharifi I, Shokrollahi H. Structural, magnetic and Mossbauer evaluation of Mn substituted Co-Zn ferrite nanoparticles synthesized by co-precipitation. *J Magn Magn Mater.* 2013;334:36–40.
11. Mahmoudi M, Sant S, Wang B, Laurent S, Sen T. Superparamagnetic iron oxide nanoparticles (SPIONs): Development, surface modification and applications in chemotherapy. *Adv Drug Deliv Rev.* 2011;63(1–2):24–46.

12. Avgoustakis K. Polylactic-Co-Glycolic Acid (PLGA). *Encycl Biomater Biomed Eng.* 2005:1–11.
13. Gaaz TS, Sulong AB, Akhtar MN, Kadhum AAH, Mohamad AB, Al-Amiery AA, et al. Properties and applications of polyvinyl alcohol, halloysite nanotubes and their nanocomposites. *Molecules.* 2015;20(12):22833–47.
14. Kumar Dutta P, Dutta J, Tripathi VS. Chitin and chitosan: Chemistry, properties and applications. *J Sci Ind Res.* 2004;63(January):20–31.
15. Parveen S, Wani AH, Shah MA, Devi HS, Bhat MY, Koka JA. Preparation, characterization and antifungal activity of iron oxide nanoparticles. *Microb Pathog.* 2018;115:287–92.
16. Liu Y, Jia S, Wu Q, Ran J, Zhang W, Wu S. Studies of Fe₃O₄-chitosan nanoparticles prepared by co-precipitation under the magnetic field for lipase immobilization. *Catal Commun.* 2011;12(8):717–20.
17. Osuna Y, Gregorio-Jauregui KM, Gaona-Lozano JG, De La Garza-Rodríguez IM, Ilyna A, Barriga-Castro ED, et al. Chitosan-coated magnetic nanoparticles with low chitosan content prepared in one-step. *J Nanomater.* 2012;2012.
18. Saeedi M, Vahidi O, Bonakdar S. Synthesis and characterization of glycyrrhizic acid coated iron oxide nanoparticles for hyperthermia applications. *Mater Sci Eng C.* 2017;77:1060–7.
19. Jadhav N V., Prasad AI, Kumar A, Mishra R, Dhara S, Babu KR, et al. Synthesis of oleic acid functionalized Fe₃O₄magnetic nanoparticles and studying their interaction with tumor cells for potential hyperthermia applications. *Colloids Surfaces B Biointerfaces.* 2013;108:158–68.
20. Seo K, Sinha K, Novitskaya E, Graeve OA. Polyvinylpyrrolidone (PVP) effects on iron oxide nanoparticle formation. *Mater Lett.* 2018;215:203–6.
21. Ruíz-baltazar A, Esparza R, Rosas G, Pérez R. Effect of the Surfactant on the Growth and Oxidation of Iron Nanoparticles. 2015.
22. Burks T, Avila M, Akhtar F, Göthelid M, Lansåker PC, Toprak MS, et al. Studies on the adsorption of chromium(VI) onto 3-Mercaptopropionic acid coated superparamagnetic iron oxide nanoparticles. *J Colloid Interface Sci.* 2014;425:36–43.

23. Paik S-Y-R, Kim J-S, Shin S, Ko S. Characterization, Quantification, and Determination of the Toxicity of Iron Oxide Nanoparticles to the Bone Marrow Cells. *Int J Mol Sci.* 2015;16(9):22243–57.
24. Hayashi H, Hakuta Y. Hydrothermal Synthesis of metal oxide nanoparticles in supercritical water. *Materials (Basel).* 2010;3(7):3794–817.
25. Method H. Chapter 2 Hydrothermal Method. 1893;18–35.
26. Wei Y, Han B, Hu X, Lin Y, Wang X, Deng X. Synthesis of Fe₃O₄ nanoparticles and their magnetic properties. *Procedia Eng.* 2012;27(2011):632–7.
27. Wu W, He Q, Jiang C. Magnetic iron oxide nanoparticles: Synthesis and surface functionalization strategies. *Nanoscale Res Lett.* 2008;3(11):397–415.
28. Mogilevskaya EL, Akopova TA, Zelenetskii AN, Ozerin AN. The crystal structure of chitin and chitosan. 2006.
29. Li Q, Dunn ET, Grandmaison EW, Goosen MF a. Applications and Properties of Chitosan. *J Bioact Compat Polym.* 1992;7(4):370–97.
30. Alvarenga ES De. Characterization and Properties of Chitosan. *Biotechnol Biopolym.* 2011;91–108.
31. Sperling R a, Parak WJ. Surface modification, functionalization and bioconjugation of colloidal inorganic nanoparticles. *Philos Trans A Math Phys Eng Sci.* 2010;368(1915):1333–83.
32. Stuart BH. Infrared Spectroscopy: Fundamentals and Applications [Internet]. Vol. 8, Methods. 2004. 224 p. Available from: <http://doi.wiley.com/10.1002/0470011149>
33. Diffraction X, Sources I. Bragg ' s Law. Production [Internet]. 1970;5(6):371–2.
34. (CFAMM) CF for AM and M. Introduction to TEM. Cent Facil Adv Microsc Microanal. 1992;1–12.
35. Zeinali S, Nasirimoghaddam S, Sabbaghi S. Investigation of the Synthesis of Chitosan Coated Iron Oxide Nanoparticles under Different Experimental Conditions. *Int J Nanosci Nanotechnol.* 2016;12(3):183–90.
36. Shen JM, Gao FY, Yin T, Zhang HX, Ma M, Yang YJ, et al. CRGD-functionalized polymeric magnetic nanoparticles as a dual-drug delivery system for safe targeted

- cancer therapy. *Pharmacol Res.* 2013;70(1):102–15.
37. Pardoe H, Chua-anusorn W, Pierre TGS, Dobson J. Structural and magnetic properties of nanoscale iron oxide particles synthesized in the presence of dextran or polyvinyl alcohol. 2001;225:41–6.
 38. Dung DTK, Hai TH, Long BD, Truc PN. Preparation and characterization of magnetic nanoparticles with chitosan coating. *J Phys Conf Ser.* 2009;187:12036.
 39. Ling Y, Wei K, Zou F, Zhong S. Temozolomide loaded PLGA-based superparamagnetic nanoparticles for magnetic resonance imaging and treatment of malignant glioma. *Int J Pharm.* 2012;430(1–2):266–75.
 40. Bolden NW, Rangari V, Jeelani S. SYNTHESIS OF DRUG LOADED IRON OXIDE NANOPARTICLES.
 41. Catalano E, Di Benedetto A. Characterization of physicochemical and colloidal properties of hydrogel chitosan-coated iron-oxide nanoparticles for cancer therapy. *J Phys Conf Ser.* 2017;841(1):1–6.

